heritage

MDPI

Article

Non-Invasive Raman Analysis of 18th Century Chinese Export/Armorial Overglazed Porcelain: Identification of the Different Enameling Techniques

Philippe Colomban [1,*], Anh-Tu Ngo [1] and Nicolas Fournery [2]

[1] MONARIS UMR8233, Sorbonne Université, CNRS, Campus P. et M. Curie, 4 Place Jussieu, 75005 Paris, France; anh-tu.ngo@sorbonne-universite.fr
[2] Galerie Nicolas Fournery, 75001 Paris, France; nf@galerienicolasfournery.fr
* Correspondence: philippe.colomban@sorbonne-universite.fr or philippe.colomban@upmc.fr

Abstract: Six rare porcelains of the Qing Dynasty, in particular, dishes ordered respectively for Philibert Orry, the Duke of Penthièvre and a tureen from the service of Louis XV, with royal coat-of-arms, were analyzed non-invasively by Raman microspectrometry. A coffee pot with a rare decoration attributed to Cornelius Pronk was also analyzed as well as two plates, one decorated with an Imari-style pattern and the second post-decorated in the Low-Countries/Holland. The enamel types and coloring or opacifying agents were identified on the basis of combined Raman and SEM-EDXS analysis previously published as well as new section and surface analysis of five plate samples representative of different technologies (blue-and-white, *Famille rose*). The use of lead oxide for the preparation of overglaze is demonstrated. For the first time, the use of borax in the blue overglaze according to the recipe from the 1753 manuscripts of French chemist Jean Hellot is demonstrated on Chinese porcelain. This fact, like the use of cobalt free of manganese, demonstrates the use of European ingredients and/or recipes for ceramics exported from China to Europe. The highlighting of the use of different recipes or raw materials for porcelain from the same period can therefore be the signature of different workshops. For instance, three different Raman signatures of red decoration were identified from the hematite vibration modes: very narrow modes for *Pronk*' coffee pot and Louis XV tureen, broad for *Orry*' dish and intermediate for the others. Three workshops are thus expected. It is interesting to note that the use of arsenic for the realization of white enamels corresponds to the latest objects, made after 1738. China was therefore in the 18th century both an importer of European know-how, design and an exporter of enameled products made with imported technologies to Europe.

Keywords: porcelain; enamel; Raman spectroscopy; SEM-EDXS; composition; cobalt; gold; arsenic; borax; hematite; import; export; *Famille rose*; *Famille verte*

Citation: Colomban, P.; Ngo, A.-T.; Fournery, N. Non-Invasive Raman Analysis of 18th Century Chinese Export/Armorial Overglazed Porcelain: Identification of the Different Enameling Techniques. *Heritage* **2022**, *5*, 233–259. https://doi.org/10.3390/heritage5010013

Academic Editor: Manuela Vagnini

Received: 30 December 2021
Accepted: 21 January 2022
Published: 23 January 2022

1. Introduction

The import of Chinese blue-and-white porcelain by the Portuguese traders in the 16th century and then on a larger scale in the 17th and 18th century by the Dutch, English, French and Swedish companies led to a craze among European elites for Chinese and Japanese ceramics [1–9], which decorations inspired in return those of the many porcelain and faience factories built in Europe in the 18th century [10–12]. In fact, the inspiration was mutual since it is now well-established both by archival [13–18] and objects [19–35] studies that the transfer of enameling technologies on metal, glass and porcelain took place at the end of the 16th century from Europe to Japan [29–31] and at the end of the 17th century to China [18–20,24–28,32–35]. Porcelains were also produced in China specifically on the order of European connoisseurs, especially decorations designed in Europe, such as those bearing coat-of-arms (armorial porcelain) [12,16,36–43]. All these objects are called '*Chine de commande*'. Important services comprising about 120 pieces were produced and

are still preserved, with various states of conservation, which allows sampling for (micro) destructive analyzes, including the examination of the sections and the stratigraphy of the enamel layers. Indeed, one of the fundamental contributions of European enameling technologies to Japanese and Chinese craftsmen is the superposition of layers of colored enamels (so-called overglaze) to obtain a complex, naturalistic decoration allowing to obtain on different supports (glass, metal or ceramic) a similar decoration to that obtained in oil painting. This technique initially developed by enamellers on metals requires strongly colored enamels (therefore, highly loaded with one or more coloring agent(s)) fired at decreasing temperatures (typically from 1000 to ~600 °C) and which can be 'painted' on a smooth, dense support, already fired, for example the glaze of a porcelain. If the realization of a complex decoration on metal is facilitated by the very short firing cycles (a few minutes plus a final annealing) and the very good-mechanical resistance of the support to thermal cycles, the enameling of ceramics is more delicate because the cycles firing must be slow and long. Many 'enamel' firing cycles are necessary, with an adjustment of the compositions of the 'overglazes' for each cycle. Produced from the reign of Kangxi, the ceramics called *Famille rose* are the first to widely use the overglaze technique.

These objects are highly appreciated by connoisseurs when they appear on art market auctions [44–49]. In some cases, the order or delivery of these porcelains is documented (such as an order for a wedding or for other important events). Besides the studies made on masterpieces to understand the use of recipes, even the ingredients imported from Europe for the realization of enameled objects in the workshops of the Imperial Palace, Jingdezhen or Canton [23,25–27] for the Court and the Chinese market, the analysis of ordered objects by European customers should make it possible to better understand the transfer of technology.

To the best of our knowledge, although reference studies on visual criteria are available [36–43], there is no systematic Raman study of the enameling technology of these export porcelains, particularly using non-invasive procedures. For two decades, Raman micro-spectroscopy has demonstrated its unparalleled potential for the non-invasive analysis of sophisticated enameled objects in the laboratory or on-site with mobile instruments [50–57]. We present here the results concerning the non-invasive Raman study of six outstanding objects (a tureen from the service of Louis XV for the Palace of Versailles, three dishes and an ewer bearing the coats-of-arms of famous historical figures and a rare coffee pot decorated with *Pronk*'s design) and two particular plates: namely, a Chinese Imari-style plate and a Dutch-decorated plate in the Kakiemon-style. In order to better validate the attributions based on previous studies of Chinese enameled porcelain [25,26,32,35], five Chinese plates (two blue-and-white, three *Famille rose*)—all these objects corresponding to the period 1700–1780, that is, from the end of Kangxi's reign to that of Qianlong—were analyzed by Raman microspectroscopy, light microscopy and SEM-EDXS on their surface and sections.

2. Materials and Methods

2.1. Methods

Valuable artefacts and fragments were analyzed in the laboratory using a Labram HR800 spectrometer (HORIBA Scientific Jobin-Yvon, Longjumeau, France) excited by an Ar^+ ion plasma laser Innova I90C 6UV (Coherent Inc., Santa Clara, CA, USA) allowing multiple wavelengths from UV to red. The 457.9 nm line is used with approximately 0.5 (dark-colored enamels) to 5 mW (paste, glaze and light-colored enamels) power of illumination at the sample surface analyzed using long working distance (LWD) 50× and 100× microscope objectives (Olympus Corp., Tokyo, Japan). Analyzed spots are about 5 × 5 and 2 × 2 μm^2; the in-depth penetration is similar for the colorless glaze, respectively. It is well-established that blue laser excitation is the most efficient to record the Raman fingerprint of glass and pottery [44–50]. However, 514.7 nm was also used but a much higher power of illumination (up to 10 mW at the sample) is required to obtain spectra with a fluorescence background at minimum level. Spectra shown in the paper have all

been recorded using the blue line. Objects are examined by focusing the laser beam on the surface or by penetrating it from a few microns to about ten microns in the coating (Figure 1). Fragments were cut from some plates having suffered accidents and then been re-glued (Table 1, Appendix A) with a diamond saw (Minitom, Struers, Ballerup, Denmark) using only pure water as a lubricant to avoid inducing fluorescence from organic pollution. The pieces cut were analyzed through the surface or on the exposed section. The recording times typically vary between 5 and 200 s with 3 to 30 accumulations made to improve the signal to noise ratio.

Figure 1. Coffee pot with *Pronk*'s design undergoing Raman analysis using a long working distance microscope (50×) objective. The analyzed spot is much smaller than the white halo.

The SEM-EDXS analysis was performed as explained in previously published works [26,55–57] with a 5510LV microscope equipped with an IXRF Systems 500 for elemental analysis (Jeol, Tokyo, Japan). The local elementary compositions expressed in oxide wt% were measured on surfaces ranging between 50 × 50 to 500 × 500 μm^2 by the calculation as implemented in the Iridium Ultra Software (IXRS System Inc., Austin, TX, USA). Boron is not measurable with this technique. The intensity of the carbon peak appears directly proportional to the roughness of the analyzed surface, this peak being minimal for smooth surfaces. Most of the carbon is thus attributed to surface pollution. The contribution of carbon to the EDXS spectrum will therefore be excluded from the quantification. Typically, the error is less than 5% for major metal oxides for a homogeneous material but reaches 5 to 20% for minor components, and much more for traces [57].

The situation is more complex for the analysis of a heterogeneous mixture, such as an enamel composed of several layers with different thickness (and composition) on a substrate in which there is a dispersion of different phases (relics, pigments, precipitates). The thickness of a coating varies from less than 1 micron for gilding to 10 to 20 microns for a layer heavily loaded with coloring agents and 100 microns or more for a light colored or transparent enamel/glaze. A measurement that is too tightly focused on a limited area will not be representative of the material, the volume of the layer generating the color being strongly disturbed by the material below. If, as is common, additions have been made to prepare the gold, they will have reacted/diffused into the substrate and even if the gold lost its former presence, it will be detected.

The volume contributing to the EDXS measurement increases in depth with the electron energy and, therefore, depends on the line used to quantify the content. The quantification software selects the most appropriate line, which is generally the K line. If this line is not optimum, the L line is taken into account by the software, etc. but it is also possible to choose another line. For example, if we consider gold, which is used for the gilding located at the very surface (thickness <1 µm), using the L line the quantification gives 8%wt and with the M line, 43%. Such differences are also observed for elements, such as lead or arsenic. We will therefore make the two quantifications for the enamels for which the EDXS spectrum shows significant peaks of heavy elements, such as Au, Pb and As. The measurement concerning these elements is therefore not very precise, both because of the very different measurement volumes depending on the peak used but also because of the long-distance diffusion of these elements and their easy loss by evaporation. If several characteristic peaks appear at the same energy and are weak (e.g., Mg and As), only that of the element which is important concerning the enameling technology will be used in order to avoid an overemphasis in its quantification.

2.2. Artefacts

The objects are presented in Figure 2, and the plates from which the samples were cut are presented in Figure A1, except for the Chinese Imari-style and the Kakiemon-style decorated plates (the later enameled in the Low-Countries/Holland), which are also presented in Figure 2. Table 1 lists the dates and dimensions; references related to identical or similar objects are also given [36–49,58–70]. The artefacts are listed according to their expected date of production in increasing order established in comparison with historical documents and dating proposed for similar artefacts [40–48,58–64].

Table 1. Studied artefacts: period of production, dimensions and references showing artefacts of the same set or similar are given. The symbols used in the rest of the text are indicated between brackets.

Artefact	Period	Description	Dimension (cm)	Figure	Procedure	References
Dish	1710–1730	Dutch decorated	D = 21	Figure 2e	Non-invasive	
Dish	1700–1720	Imari style	D = 22	Figure 2f	Sampling	
Ewer	1720–1725	*Duvelaer* family coat-of-arms	H ~25	Figure 2a	Non-invasive	
Dish	circa 1730	*Philibert Orry* coat-of-arms	D = 25	Figure 2g	Non-invasive	[48,59]
Dish	1730–1735	*La Bistrate*-and-*Poli* family coat-of-arms	D = 22	Figure 2d	Non-invasive	[60,63]
Dish	circa 1737	*Duc de Penthièvre* coat-of-arms	D = 22.5	Figure 2h	Non-invasive	[62]
Tureen	circa 1738	Louis XV table set with the coat-of-arms of kings of France		Figure 2c	Non-invasive	[42–47,61]
Coffee pot	1730–1740	*Pronk*' design	H = 34	Figures 1 and 2b	Non-invasive	[58,65,66]
Plate (LA)	1740–1750	Mountainous river landscape decor (*Famille rose*)	D = 22	Figure A1c and Figure 3c'	Sampling	[26]
Plate (PEO)	circa 1760	Citrus and peony pattern (*Famille rose*)	D = 23	Figure A1	Sampling	
Plate (Rose)	circa 1770	Rose pattern (*Famille rose*)	D = 23	Figure A1e	Sampling	
Cup saucer (BW f)	circa 1780	Floral pattern (*Blue-and-white*)	D = 12	Figure A1a	Sampling	[55]
Plate (BW ww)	circa 1780	Weeping willow pattern (*Blue-and-white*)	D = 23	Figure A1b	Sampling	

Figure 2. (**a**) Ewer with the *Duvelaer* coat-of-arms; (**b**) coffee top with *Pronk*'s design; (**c**) tureen from the service of Louis XV bearing the royal coat-of-arms; (**d**) plate with the *la Bistrate*-and-*Proli* family coat-of-arms; (**e**) Dutch-decorated plate with Kakiemon-style pattern; (**f**) Imari-style Chinese plate; (**g**) plate with *Philibert Orry*' coat-of-arms; (**h**) plate with the *Duc of Penthièvre*' coat-of-arms.

- A dish of rounded form made in China and later enameled in Holland assigned from the end of Kangxi or Yongzheng reign, with a Kakiemon-style design of two quails pecking at millet beneath flowering stems, a grasshopper perched above, the rim with four panels of quail within a cracked ice and prunus ground in a *Famille verte* palette (Figure 2e). This unusual but well-executed design once again demonstrates the confusion that Dutch decorators held over the source of oriental decoration, combining elements of Japanese and Chinese designs on one plate to produce an attractive, but distinctly European, effect;
- A Chinese 'Imari' plate, Kangxi period (1662–1722), ca. 1700/1720 (Figure 2f). Decorated in the Imari-style as original Japanese porcelain made at kilns at/near Arita, (Hizen province), with Buddhist wheel, scrolling lotus, chrysanthemum and peony sprays with their foliage;

- A rare Chinese ewer (Figure 2a), Kangxi period, probably ca. 1720/1725. Modeled after a European silver shape with an incurving bracket handle, spreading foot and molded human mask with a beard under the spout, enameled around the body camellia branch above molded elongated petals reserved on a seeded-green ground, the foot with similar decoration. The body is decorated with the coat-of-arms of the *Duvelaer* family. Members of this family lived in Holland, Austrian Low-Countries and France during the 18th century. The shape of a stick ewer was in vogue in France between 1700 and 1725. Afterwards, it was out of fashion (so it is almost impossible that it had been ordered after that date);
- A Chinese armorial dish for the French market (Figure 2g), Yongzheng period (1723-1735). With the coat-of-arms of *Orry* family, *de gueule à un lion rampant et grimpant sur un rocher d'argent*, in colors and gilt with a *rocaille* surrounded by a vividly enameled foliate border, the rim scalloped. *Orry* was named *Contrôleur général des finances* (Royal Finance Minister) in 1730 and combined this function with being the general director of the *Bâtiments du roi* (The royal buildings office) in 1736, after the death of the *Duc d'Antin*. *Orry* remained *Contrôleur général* until 1745, making him the longest continuously serving holder of the office in the 18th century.

One of *Philibert Orry*'s parents was Father *Louis-François Orry*, procurator of the missions of China and India, with whom Father *d'Entrecolles* had correspondence on the technical precedents and elaboration of Chinese porcelain between 1712 and 1722 in Jingdezhen. The decor seems stylistically to be early but still very *Regency* (and not *Rocaille*). A dating around 1730 appears to be reasonable, although other arguments may be in favor of a later date, such as 1740–1745 [42,43,48,59];

- A Chinese export *Famille rose* and silvered armorial plate (Figure 2d) for the Belgian market (*la Bistrate* of Anvers) [60,63], Yongzheng period, i.e., before 1735. The center enameled and silvered with the arms of *la Bistrate accollée* with those of *Proli* (his wife' Family) between greyhound supporters and below, a helmet, a coronet and a coat-of-arms, surrounded by a trellis-pattern in the well, the arms repeated individually around the everted rim between a *du Paquier* style design of linked feathers, strapwork, shells and hanging drapery. This service was made for *Jean-Charles de la Bistrate* (baptized in Anvers in 1715), seigneur de Loer and Neerwinde and chief almoner of Anvers who married *Anne-Martine Proli* (born in 1711), also of Anvers on October 7, 1736. Her father, *Pierre Proli*, was one of the seven directors of the *Compagnie d'Ostende.* Objects bearing the same coats-of-arms are also known [60–63]. *La Bistrate's* wedding took place in October 1736. Stylistically, we would wish to assign it earlier, around 1730, but this is almost impossible since the marriage of the future spouse could not have been planned six years in advance. The order must have been made around 1734/1735, to allow for the time that the order reached China and then the service traveled from China to Europe;
- A Chinese armorial dish for the French market, Yongzheng period, ca. 1730 [62]. Decorated in the *Famille verte* palette, with the coat-of-arms of *Penthièvre*. The order depicted with the coat-of-arms is Knight of the Golden Fleece and the Holy Spirit as well as the Anchor of Admiral of the Fleet. The service was order for Louis-Jean-Marie de Bourbon, *Duc de Penthièvre*, *de Chateuvillain*, *de Rambouillet*, (1725–1793), his father, the *Comte de Toulouse*, son of King Louis XIV [62]. Stylistically, this service is early; the wing is in the style of the *Famille verte*, the decoration employing this red color is so particular that we date today around 1730, although the marine anchors give a broad dating of the order;
- A Royal armorial tureen for the French market, Qianlong period (1736–1795), ca. 1737–1740 (Figure 2c). Decorated with the royal coat-of-arms of France, the reserve and sides below the underglaze-blue shell-form handles with a Buddha's hand citron or a gourd in a dish on a lotus blossom, and pads or branches, the rim with a floral-scroll border repeated around the chrysanthemum-decorated know three gilt *fleurs-de-lus* alternating with floral roundels. This service was delivered at Versailles, for the winter

dining room of King Louis XV of France [42–46,61] in 1740 through the French East India Company for the Palace of Versailles;

- A rare *Pronk*' design coffee pot and cover (Figures 1 and 2b), Qianlong period, ca. 1740. Painted with a wide band of beetles, butterflies and moths above black-ground flowering vine, all between a mint-green scale pattern, the black-ground with gilt tassel or bell-flower motifs. *Cornelis Pronk* was a Dutch draughtsman [64–66], who was commissioned by the directors of the Dutch East India Company from circa 1734–1738 to produce designs to be transferred onto Chinese porcelain. Compared to the other known pieces [58], the porcelain handle has been replaced by a silver handle;
- Four plates, a cup and saucer were analyzed on their surfaces (non-invasively) and on sections prepared by diamond saw cutting: two blue-and-white porcelains, Qianlong period, circa 1780, one depicting a floral décor (Appendix A, Figure A1a), the second a weeping willow décor (Appendix A, Figure A1), and three *Famille rose* porcelains, depicting a 'mountainous river landscape' (Appendix A, Figure A1c,c'), circa 1740–1750, citrus and peony (Appendix A, Figure A1d), circa 1760, and a rose (Appendix A, Figure A1e), circa 1770, respectively.

3. Results

Figures 3–6 show details of surface and section optical photomicrographs of the Imari-style and the *Famille rose* plates at different magnification. Information on the stratigraphy is required to fully interpret the EDXS and Raman data, especially when they are recorded on the object from the top surface (Figure 1). Photomicrographs obviously show that colored areas were coated on the colorless glaze. The variable distribution of the color (and coloring agents/pigments) is obvious. In some places, the coating forming black and red lines has been lost (e.g., Figures 3 and 4).

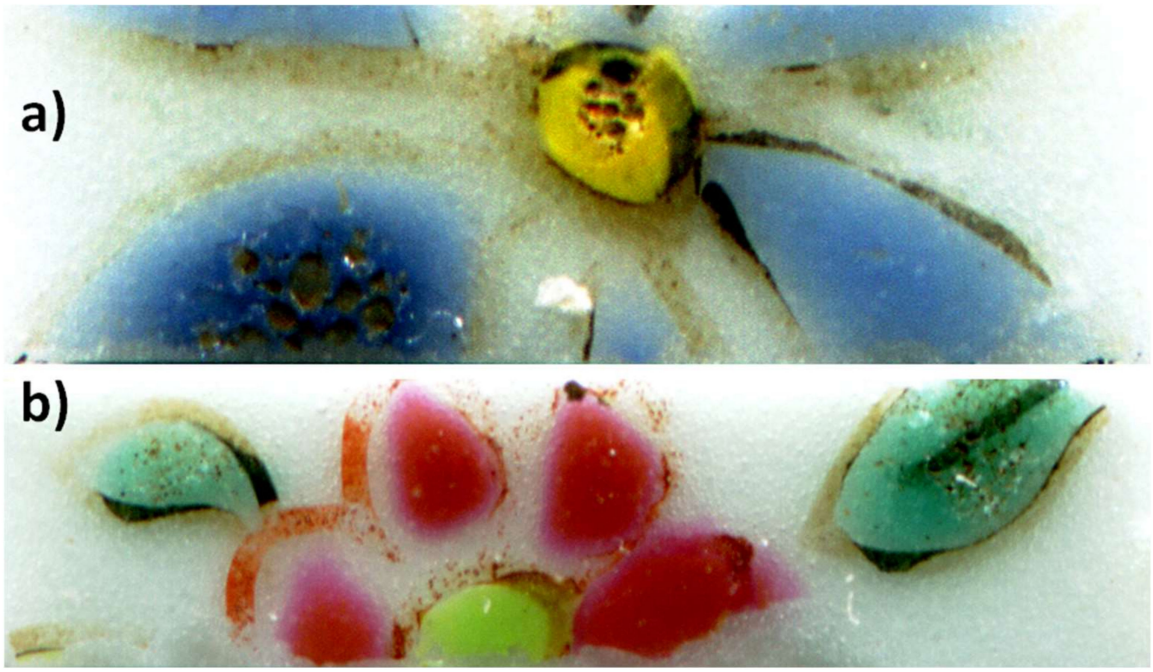

Figure 3. Detail view of the décor of Rose plate (20 × 4 mm^2, each, see Appendix A, Figure A1e): yellow, blue, red, pink, green, black overglazes and colorless glaze of areas depicting blue (**a**) and red (**b**) flower (see corresponding elemental composition in Tables 2 and 3).

Table 2. Local oxide 'compositions' (oxide wt%) of the body and glaze measured by SEM-EDXS on reference shards; the magnification used is given; metal wt% for gold; nd: not detected. Numbers in italics have been obtained by manually selecting the most suited Pb line for quantification. Most characteristic values are in bold font.

Artefact (Magnification)	Spot	SiO_2	Al_2O_3	MgO	TiO_2	Na_2O	K_2O	CaO	MnO_2	Fe_2O_3	CoO	CuO	ZnO	PbO	Au
BW ww (200×)	body	65.6	28.2	0.6	0.02	2.9	1.6	0.7	0.8	0.3	0.02	nd	nd	nd	nd
BW f (200×)	body	66.2	29.9	0.5	0.03	1.35	1.1	0.5	0.9	0.2	0.02	0.06	0.05	nd	nd
Imari (150×)	body	66.8	27.8	0.8	0.05	1.9	1.7	0.4	0.05	0.3	0.03	0.05	0.05	nd	nd
LA (150×)	body	67.1	27.6	0.8	0.02	2.1	1.5	0.4	0.05	0.4	0.02	0.05	0.05	nd	nd
BW f (200×)	Glaze(blue)	71.4	21.6	0.5	0.1	1.3	1.9	1.4	0.9	0.5	0.1	0.15	0.15	nd	nd
BW ww (200×)	Glaze(blue)	69.1	21.8	0.5	0.02	3.1	1.4	3.1	0.5	0.3	0.1	nd	nd	nd	nd
LA (150×)	Glaze (blue)	70.7	22.2	0.5	0.05	2.1	1.4	1.4	0.9	0.5	0.1	0.1	0.07	nd	nd
LA (400×)	Glaze (blue surf)	73.2	**14.9**	0.7	0.05	1.1	**4.5**	**4.5**	0.05	0.7	0.08	0.1	0.09	nd	nd
BW ww (1000×)	Defect (white)	**59.2**	17.8	1.7	0.03	1.	0.5	**15.3**	0.38	3.5	0.1	0.1	0.2	nd	nd
BW ww (1000×)	Defect (black)	**30.3**	**11.4**	1.2	0.04	0.5	0.2	10.7	0.7	**43.2**	1.2	0.1	0.2	nd	nd
Imari (50×)	Glaze (close to gilding)	66.6	24.5	0.2	0.15	1.5	0.4	2.2	0.13	0.8	0.07	0.26	0.13	**1.5**	**1.5**
Rose (50×)	Glaze1B?	*62.7*	*22.1*	*0.5*	*nd*	*4.3*	*1.2*	*0.9*	*0.03*	*0.5*	*0.02*	*nd*	*nd*	***8***	nd
Rose (50×)	Glaze 2	*64.6*	***15.4***	*0.5*	*nd*	*3.1*	*1*	***2.8***	*nd*	*0.3*	*nd*	*0.1*	*nd*	***12.2***	nd

Table 3. Local oxide 'composition' (wt%) measured by SEM-EDXS on colored enamels; the magnification used is given (metal in wt% for gold and silver; nd: not detected, for any characteristic peak visible in the spectrum). Elements belonging to the chromophore/pigment are written with an underlined bold font. Values in italics are obtained by choosing M line for heavy elements.

Artefact (Magnification)	Spot	SiO_2	Al_2O_3	MgO	TiO_2	Na_2O	K_2O	CaO	MnO_2	Fe_2O_3	CoO	CuO	ZnO	As_2O_5	PbO	Au[Ag]
BW ww (200×)	Blue	71.7	18.1	0.5	0.1	2.8	1.5	4.0	0.7	0.5	**0.1**	nd	nd	nd	nd	nd
	Blue 3	69.1	21.8	0.55	0.02	3.1	1.4	3.1	0.5	0.3	**0.1**	nd	nd	nd	nd	nd
Rose (50×)	*Blue*	*62.3*	*4.9*	*nd*	*nd*	*3*	*1.7*	*0.2*	*0.1*	*0.3*	***0.03***	*nd*	*nd*	*1.2*	*26.1*	*nd*
	Blue inter	*60.2*	*22*	*nd*	*nd*	*3.2*	*0.9*	*0.5*	*0.05*	*0.5*	***0.1***	***1.6***	*nd*	*1.1*	*10*	*nd*
Imari [Pb L]	Blue	57.9	20.6	0.3	0.25	5.9	1	5.2	0.35	1.3	**0.1**	0.35	0.25	0	3.4	1.
(50×) [Pb M]	"	*45.1*	*16.5*	*nd*	*nd*	*3.5*	*1*	*4*	*nd*	*nd*	***nd***	*nd*	*nd*	*0.8*	*16.7*	*nd*
Rose (50×)	Blue	*60.2*	*22*	*nd*	*nd*	*3.2*	*0.9*	*0.5*	*0.05*	*0.5*	***0.1***	***1.6***	*nd*	*1.1*	*10*	*nd*
[Pb L]	"	*62.3*	*4.9*	*nd*	*nd*	*3*	*1.7*	*0.2*	*0.07*	*0.3*	***0.03***	*nd*	*nd*	*1.2*	*26.1*	*nd*
[Pb M]	defect	*61.2*	*11*	*nd*	*nd*	*1.1*	*1.4*	*1.1*	*0.1*	*0.4*	***0.06***	*nd*	*nd*	*2.3*	*21.3*	*nd*
LA (35×)	Green	86.6	8.4	nd	0.06	2.3	0.5	0.3	0.06	0.3	0.02	**1.2**	nd	0.7	0.6	nd
PEO (50×)	Green	88.2	6.1	nd	0.04	2.2	0.7	0.5	nd	0.5	nd	**0.2**	nd	0.9	0.6	nd
	"	*49.4*	*3.5*	*nd*	*0.02*	*1.2*	*0.4*	*0.3*	*nd*	0.3	nd	**4.4**	nd	0.5	39.9	nd
Rose (50×)	Green	55.3	6.4	nd	nd	1.2	0.6	0.7	0.1	0.5	0.08	**4.6**	nd	0.3	30.3	nd
	Yellow-green	71.6	10.3	nd	nd	1.7	0.3	0.3	nd	0.2	nd	0.1	nd	nd	**15.1**	nd
LA (35×)	Yellow	85.3	10.2	nd	0.02	2.2	0.4	0.2	0.07	0.3	0.04	0.15	nd	0.6	**1**	nd
	"	*64.2*	*7.7*	*nd*	*0.01*	*1.6*	*0.3*	*0.1*	*0.05*	*0.2*	*0.03*	*0.09*	*nd*	*0.4*	***25.2***	*nd*
Rose (50×)	Yellow [(a)]	*67.2*	*15*	*0.3*	*nd*	*2*	*0.4*	*0.2*	*nd*	*0.7*	*nd*	*0.2*	*nd*	*nd*	***13.4***	nd
Imari (50×)	Red	59.8	22.1	0.02	0.2	1	1.1	2.6	0.1	**9.9**	0.3	0.2	0.18	0	1.6	**1**
	"	*38.8*	*15.2*	*0.01*	*0.15*	*0.6*	*0.7*	*1.8*	*0.08*	***6.3***	*0.2*	*0.15*	*nd*	*0.7*	*34.5*	***0.6***
LA (35×)	Red/gold	64.6	22.6	0.5	nd	4.6	0.6	2.4	0.1	0.6	0.1	nd	nd	**2**	0.5	**2**
	"	*54*	*21.2*	*nd*	*0.04*	*3.7*	*0.6*	*2*	*0.1*	*0.5*	*0.1*	*nd*	*nd*	***2.2***	*15.5*	***0.5***
	Red/	58.8	2.3	nd	0.05	1.7	1.2	0.1	nd	0.3	nd	nd	nd	**0.8**	33.8	**1**
	Red/pink	87.6	3.5	nd	*nd*	2.7	1.8	0.1	0.1	0.5	*nd*	*nd*	*nd*	**1.1**	1.8	**2**
		66.5	*4.3*	*nd*	*0.1*	*1.8*	*0.5*	*0.1*	*0.05*	*0.4*	*0.03*	*nd*	*nd*	***2.5***	*23.7*	**2**
	Pink-white	80.4	7.5	nd	0.03	2.1	0.2	0.2	nd	0.6	nd	nd	nd	**10.0**	1	nd
		68.8	*6.4*	*nd*	*0.03*	*1.8*	*0.16*	*0.2*	*nd*	*0.5*	*nd*	*nd*	*nd*	***7***	*15.1*	*nd*
	Dark pink	73.2	15.1	nd	0.1	4.4	0.5	0.9	0.13	0.3	nd	nd	nd	**4.7**	1	**1**
		57.7	*12.1*	*nd*	*0.1*	*3.5*	*0.4*	*0.7*	*0.1*	*0.2*	*nd*	*nd*	*nd*	***3.9***	*21.1*	***1***

Table 3. *Cont.*

Artefact (Magnification)	Spot	SiO_2	Al_2O_3	MgO	TiO_2	Na_2O	K_2O	CaO	MnO_2	Fe_2O_3	CoO	CuO	ZnO	As_2O_5	PbO	Au[Ag]
LA (50×)	Pink	*56.2*	*2.7*	*nd*	*nd*	*1.7*	*1.9*	*0.2*	*nd*	*0.3*	*nd*	*nd*	*nd*	***1.4***	*34*	***1***
Rose (50×)	Pink	*52.4*	*2.1*	*nd*	*nd*	*1.5*	*2.2*	*0.1*	*nd*	*0.2*	*nd*	*nd*	*nd*	***0.4***	*40.1*	***1***
	Pink-red	*61.6*	*14.7*	*0.5*	*nd*	*3.7*	*0.7*	*2.6*	*nd*	*0.2*	*nd*	*1.5*	*nd*	*nd*	*14.3*	***0.5***
PEO (100×)	White	72.8 *52.4*	11.8 *8.7*	nd nd	0.02 0.02	2.3 1.7	0.6 0.4	0.2 0.1	nd nd	nd 0.1	nd	nd	nd	**11.9** **9.3**	0.3 39.9	nd *nd*
LA (35×)	White	80.4	7.5	nd	0.02	2.1	0.2	0.2	nd	0.6	nd	nd	nd	**10.0**	1	nd
Imari (50×)	White "	66.4 *47.9*	24.4 *18.7*	0.2 *0.1*	0.15 *0.1*	1.5 *1.1*	0.4 *0.3*	2.2 *1.7*	0.13 *0.1*	0.8 *0.6*	0.07 *0.04*	0.26 *0.2*	0.13 *0.1*	0 ***0.8***	1.5 *27.8*	1.6 *nd*
LA (50×)	White 1	*60*	*5.9*	*nd*	*nd*	*1.2*	*0.9*	*0.6*	*nd*	*0.7*	*nd*	*nd*	*nd*	***6***	*24*	*nd*
	White 2	*38*	*1.7*	*nd*	*nd*	*1*	*2.9*	*0.2*	*nd*	*0.4*	*nd*	*nd*	*nd*	***4.1***	*51.7*	*nd*
BW ww (1000×)	Black defect	30.3	11.4	1.2	0.04	0.5	0.2	10.7	0.7	**43.2**	1.2	0.1	0.2	*nd*	*nd*	*nd*
Rose (50×)	Black [(b)]	*47*	*2.5*	*nd*	*nd*	*1.7*	*0.6*	*0.6*	*nd*	*0.6*	*nd*	*4.7*	*nd*	*nd*	*42.3*	*2*
Imari (50×)	Gilding	*25.3*	*4.4*	*0.02*	*0.1*	*0.3*	*0.6*	*3.1*	*0.2*	*5.6*	*0.3*	*0.45*	*0.4*	*3*	*9.8*	***46[3]***
LA (35×)	Gilding	*60.1*	*13.7*		*0.05*	*2.7*	*0.6*	*4.9*		*1*	*nd*	*nd*	*nd*	*1*	*15.7*	
LA (35×)	Gilding S	*24.1* *11.1*	*4.5* *2.3*	*nd* *nd*	*0.3* *0.1*	*1* *0.5*	*0.9* *0.5*	*5.0* *2.9*	*0.1* *0.06*	*2.6* *1.4*	*nd* *0.1*	*nd* *nd*	*nd* *nd*	*1.5* *0.1*	*2* *16.4*	***53[6]*** ***60[3]***
PEO (50×)	Gilding	*23.2*	*4.1*	*nd*	*nd*	*0.6*	*0.3*	*2.7*	*0.2*	*2.7*	*nd*	*nd*	*nd*	*0.5*	*24*	***38.9[2.9]***

[(a)] Tin and antimony detected (SnO_2:0.6, Sb_2O_5:0.05 wt%); [(b)] high carbon peak.

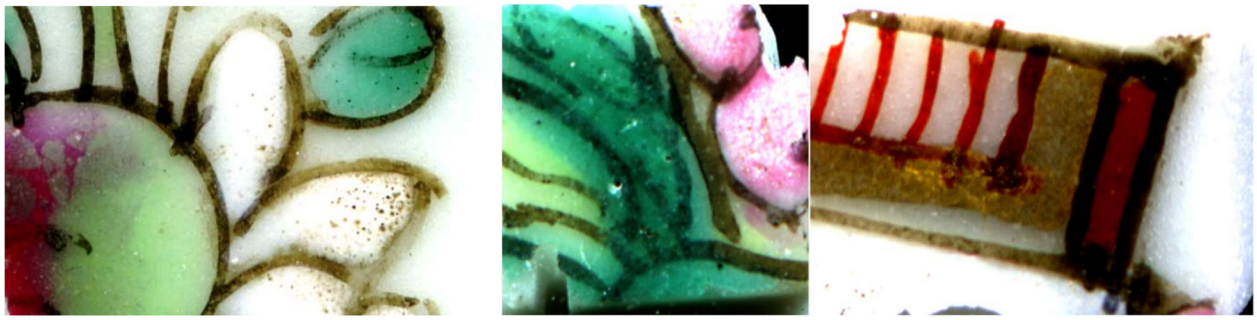

Figure 4. Detail view of the décor of LA plate (4 × 4 and 4 × 8 mm^2, respectively, see Appendix A, Figure A1c,c'): green, pink, red, white and black overglazed, gilding and colorless glaze (see corresponding elemental composition in Tables 2 and 3).

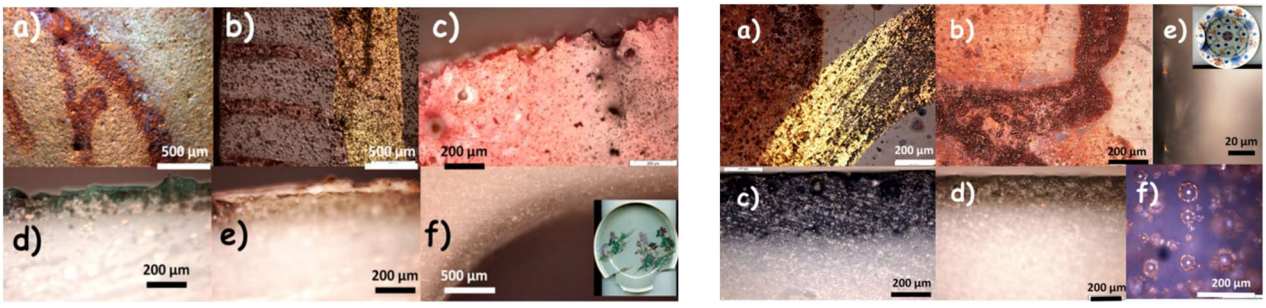

Figure 5. Surface and section optical view of **left**, a *Famille rose* plate with a landscape decoration (LA, **a**,**b**,**d**–**f**: section view; **c**: top view; see Appendix A, Figure A1c) and **right**, the Imari-style plate (**a**,**b**: top view; **c**–**f**: section view; see Figure 2f).

Section views (Figures 5 and 6 and Appendix A, Figure A2) show the typical thickness of the glaze and overglazes: circa 200 to 500 µm for the glaze and 30 to 100 µm for the overglaze. Note that the thickness of the gold foil applied is much thinner, less than a few microns (Figure 5e-right) and the covering of the surface with gold is far from complete (Figure 5a,b-left; Figure 5a-right). Consequently, Raman measurements made on

the gilded area will give information on the reaction layer associated with the gilding and thus elements associated with the preparation and use of gold. With the 50× and 100× microscope objectives used in the study, the volume analyzed is less than ~200 and 10 μm^3. In the same way, the EDXS measurement will depend on the coverage rate by the gold particles of the analyzed area and the magnification. Thus, the 'composition' obtained by quantification of the spectrum will depend on the elements distributed heterogeneously in the analyzed volume.

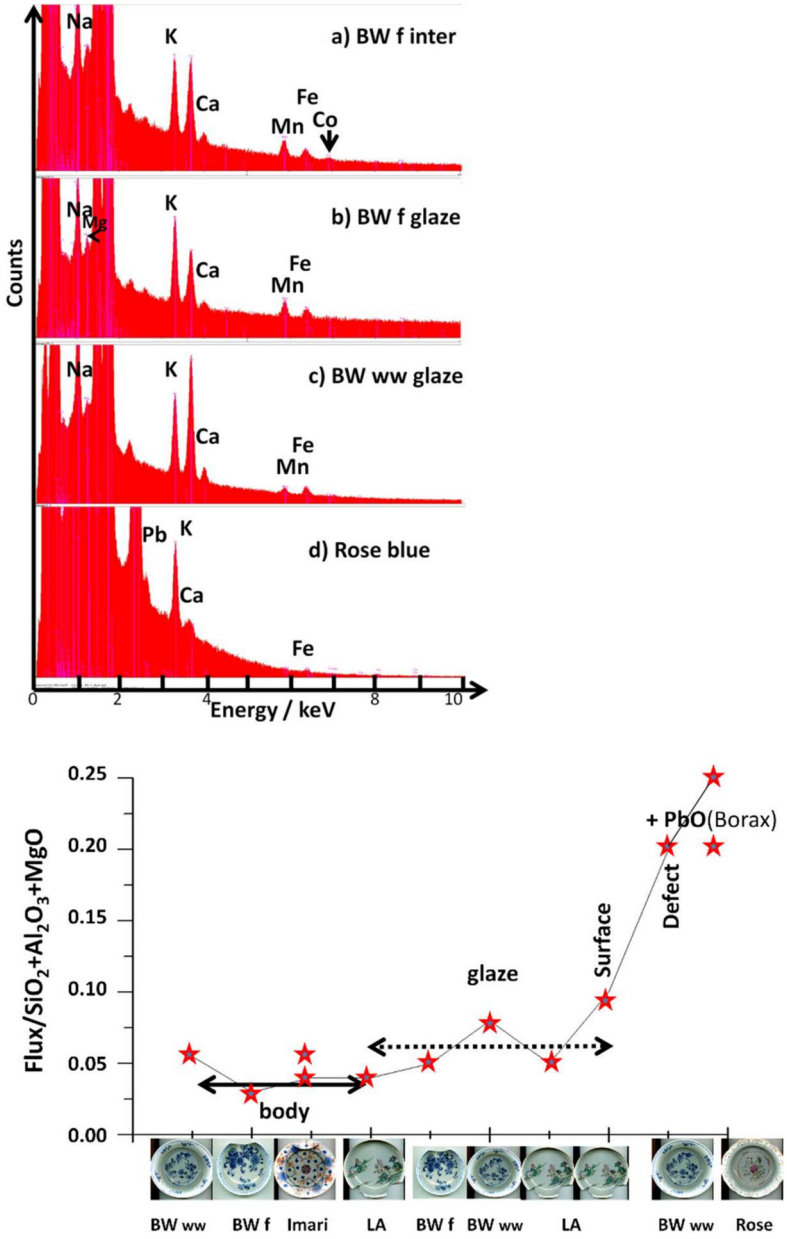

Figure 6. Comparison of the fluxes ($Na_2O+K_2O+CaO+PbO$) vs. polymerized network (SiO_2 + Al_2O_3 + MgO) oxide wt% ratio for body, glaze and glaze defects. Details of EDXS spectra are given for BWf (**a**, body-glaze blue interphase and **b**, blue glaze), BWww (**c**, blue glaze) and Rose (**d**, blue overglaze) artefacts: The intensity has been increased to allow comparison of the contents of flux (sodium, potassium, calcium and lead) and transition metals providing color (manganese, iron).

Bubbles are observed at the surface of many overglazes (e.g., Figures 3 and 4). The formation of bubbles is promoted by addition of carbonates, borax, reaction with the substrate and overheating of the glaze.

Areas analyzed by SEM-EDXS have been selected after the analysis by Raman microspectroscopy (and sampling the plates), which allowed the determination of the areas that are representative of various characteristic Raman signatures. For a more didactic presentation, the elemental 'composition' will be presented first.

Figure 6 compares Raman and representative EDXS spectra selected among various analyzed spots of glazed areas of different pieces sampled from the plates shown in Figure A1. The total flux and corresponding Na_2O, K_2O, CaO and PbO contents are compared in Figure 7. Figure 8 shows representative spectra recorded on the Imari-style plate.

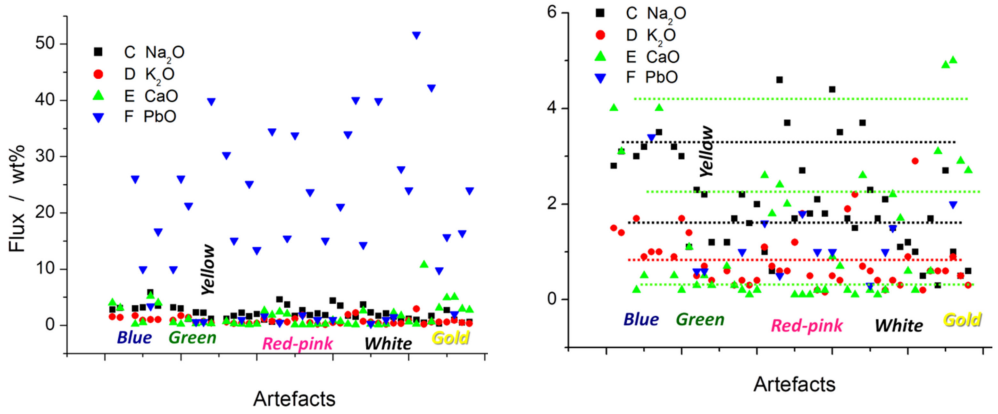

Figure 7. Comparison of the Na_2O, K_2O, CaO and PbO wt% for the different overglazes (data are given from left to right according to the order in Table 3, from the top to the bottom). A zoom is given on the right.

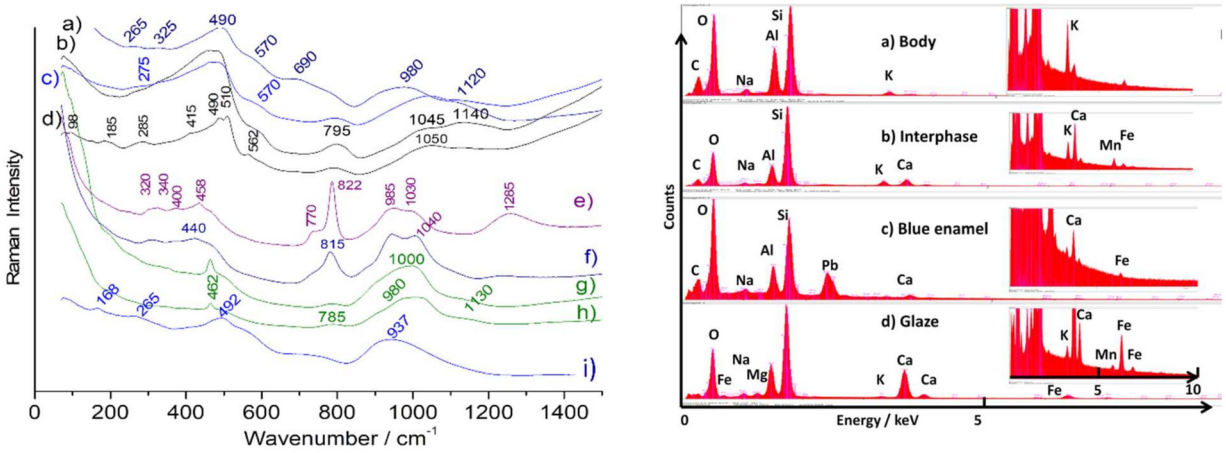

Figure 8. Representative Raman spectra (**left**) and EDXS spectra (**right**) recorded on various areas of enameled/glazed porcelains. **Left**: **a**–**i**, Raman spectra recorded on blue (**a**,**b**) and colorless (**c**) glaze of blue and white artefacts (Figure A1a,b); (**d**) spectra recorded on the glaze–body interface (Figure A1b); (**e**,**f**) spectra recorded on the blue petal of a flower of *Famille rose* plate depicting a rose (Figures A1e and 3a: **e**, petal periphery, **f**, petal centre); (**g**,**h**) spectra recorded on green overglaze (plate, Figure A1d); (**i**) spectra recorded on the non-colored area of a black dot defect (Figure A1b). **Right**: (**a**) EDXS spectra of porcelain body and (**b**) glaze-body interphase (LA, Figure A1e plate); (**c**) blue glaze of Imari-style plate (Figure 2f); (**d**) glaze of blue-and-white (BW ww) porcelain (Figure A1b).

3.1. Compositions

Table 2 compares the 'compositions' of the body and colorless glaze measured on the pieces cut from the plates shown in Figure A1. Comparison of the 'composition' of colored areas is made in Table 3.

Silica and alumina contents measured on the body are very similar and small differences can arise from the contribution of quartz grains in the volume probed by the electron beam. Differences are more explicit regarding the Na_2O content. The error for the calculation of the trace element content [CoO, CuO, and ZnO] is expected to be large, and the lower values measured can be considered as an indication of the 'limit of reliable detection' (LORD). Consequently, only values measured greater than 5 to 10 times of this LORD will be considered as representative and the quantification is not made for all samples.

The 'composition' measured on the glaze shows significant differences. The greatest difference is measured in the analysis of a defect (a black point), which shows a separation under the microscope occurring between a non-colored phase and a black phase very rich in iron oxide (43 wt%). Despite the magnification used (1000×), this measurement is undoubtedly significantly contaminated by the neighboring non-colored phase since the SiO_2/Al_2O_3 ratio remains identical to that of this phase. The non-colored phase is very rich in lime which proves that a very rich calcium phase had been used in the preparation of the enamel (calcite or chalk) and the defect was probably caused by a poor grinding procedure.

Even far from the colored areas, pollution by lead oxide was detected for plates that possess overglaze decoration. In fact, lead oxide is very volatile above 850 °C and contaminates all the objects in the same heating batch.

The level of cobalt in the blue glaze is 10 times higher than in the paste (equal to the LORD), but intermediate values were measured in the colorless glaze that raises the question of a whitening of the glaze achieved by a small addition of cobalt. Measurements with more precise methods for trace analysis are needed to confirm this hypothesis. Differences in the concentration of certain flux oxides between the surface layer and the body of the glaze layer are also observed, as already have been made for some Ming blue-and-white porcelains [55]. The composition of the glaze of the Imari-style plate is distinguished by its low potassium content as for BW ww plate (Table 1, the symbols BW ww, LA, etc. are explained in the Table). This confirms the previous study on Ming blue-and-white export porcelains [55] that many glaze compositions had been used simultaneously.

Examination of Table 3 comparing the EDXS measurements made on colored areas separates the objects into two groups, as expected. The first group includes blue-and-white objects and the other one covers the objects with multicolored decoration where overglazes contain PbO. The blue areas of the two blue-and-white porcelains are slightly different in composition from the colorless glaze, with less alumina, more CaO and unsurprisingly more CoO (~0.1 wt%). This indicates that chalk and silica were added with cobalt to produce the décor. The analysis of the cross sections (Figure 2) shows that the blue decoration was drawn on the paste in a clear way for BW ww plate (blue underglaze). Cross section views of the BW f samples show that the blue color looks homogeneous in all the section of the glaze (Appendix A, Figure A2). However, the EDXS measurement at the body–glaze interface (BW f inter section, Figure 6-left) shows that the intensity of tiny Co Kα peak is slightly higher that is consistent with a blue décor drawn on the green body. This difference can come from the deposit of the glaze on a still damp blue décor and the greater fusibility of this glaze. Figure 6 also compares the different ratios for the flux vs. refractory oxides forming the polymerized network. The value measured for the colorless glaze is not very different from the mean value measured for the bodies because both were fired simultaneously.

Larger values were measured for the defects or in the case of lead polluting the glaze (measurement at the very surface) and of course for overglazes. Note that the peak of Mn is higher in the BW f than in the BW ww glaze (Figure 6-left). No Mn and a very low level of Fe were detected in the Rose blue overglaze (see further).

Figure 7 compares the flux oxide content for the various overglazes. Except for rare colors (red or white, both associated with arsenic), the CaO content is always low (<0.2 wt% CaO) and the K_2O content is ~1 wt%. The Na_2O content is higher and two groups are obvious (~2 and 3–4 wt%).

The PbO content is very variable, from 0 to ~50 wt% and the quantification depends on the line used. Part of the variability arises from the volatilization–condensation process close to the lead-based overglaze but also reflects the uncertain character of the measurement for this element. The oxide content of the coloring agents (transition metals, gold nanoparticles, arsenic- and tin-based opacifiers) should be considered as a confirmation of the use of the detected element and not as a representative composition of the overglaze. However, the local oxide composition depends on the spot (a decoration requires the variation of the distribution of chromophores in an xy plane and along the z direction), but also is affected by the intrinsic weaknesses of the measurement technique (the in-depth probed is a function of the electron/photon energy and the used magnification). Among the detected elements, it appears obvious that Co is the blue chromophore, Cu the green one (Figure A3c) and gold the chromophore for rose to (red-)pink colored areas. The level of gold detected in pink to red overglazes is small, 0.5 to 2 Au wt% (Table 3).

Yellow to green colors were produced with lead-based pigments and their characterization is only possible by Raman scattering. A rather high level of arsenic (As_2O_5: 4 to 10 wt%) was measured in the (opaque) white overglazed areas. Tin and traces of antimony were clearly detected in one of the overglazed areas (yellow, Rose plate, Figure A1e). These coloring elements have been already identified in *Famille rose* porcelains [19,20,23,26,27]. Gold used in the gilding contains a small amount of silver (5 to 10 wt%, see Table 3 and Figure A3) as is commonly observed. Silver was probably used to promote the adhesion to the glaze substrate [32,71].

3.2. Characteristic Raman Signatures

3.2.1. Body

Raman spectra recorded from the porcelain body indicate quartz (α–SiO_2) with a characteristic strong SiO_4 bending mode at ~463 cm^{-1}, somewhat shifted down a few cm^{-1} under the compressive stress of the mullite and glassy matrix due to the lower thermal expansion of the latter phases [50,54–56,72]. The spectrum of almost pure acicular mullite ($3Al_2O_3$ 2 SiO_2) can also be identified in some spots with rather narrow components at ~600, 960 and 1140 cm^{-1} (Appendix A, Figure A4-left and Figure A5-right), the two later very characteristic of SiO_4 stretching modes [54,73,74]. Sometimes, we also observe weak components at 230 and 415 cm^{-1}, characteristic of cristobalite (SiO_2) formed by the transformation of the quartz grains reacting with the flux [72]. Finally, as shown in spectrum d, Figure 8, the main peak of feldspar/plagioclase is seen at ~510 cm^{-1} and smaller associated peaks at 95, 190 and 560 cm^{-1} [50,55] can also be observed in the glaze, body and the interface. The different bodies exhibit a very similar Raman signature and the comparison of the phase amount by unit surface should be made to extract quantitative differences. This is consistent with the observation of rather similar compositions (Table 2) with the main difference in the MgO content. However, no Mg-based crystalline phases were detected and a low Mg content does not have a visible influence on the Raman spectrum of the glassy phase because of the high ionicity of the Mg-O bond. As a conclusion, information that could be obtained by the Raman analysis of objects from spectra recorded on the body will be limited. Thus, we will focus the work on the Raman analyses of the glaze and overglazes.

3.2.2. Glaze and Overglazes

In contrast, a large variety of spectral signatures is observed regarding the Raman spectra recorded on the glaze and overglazes (Figure 8). Compositional variations are also obvious from the elemental analyses, especially regarding the calcium content for the glaze, and the arsenic and lead contents for the overglaze. Indeed, as recently demonstrated in the study of Ming blue-and-white porcelain glazes [55] two signatures are currently observed for blue-and-white porcelain: (i) one signature is characterized with the strong and broad band at ~480 cm^{-1} and (ii) a doublet of small intensity at ~1050–1130 cm^{-1} (b-Raman spectrum in Figure 8) and another characterized by two bands of rather similar

intensity, at ~500 and 980 cm^{-1} (a spectrum in Figure 8). The first is associated with a glaze in which the sodium, potassium and calcium contents are low (and consequently their peaks on the EDXS spectra have a similar small height, see b-interphase spectrum in Figure 8). The second type of glaze is richer in calcium (see Figure 8-left g–i), with a composition rather similar to that of celadons (Ca-rich) [75–79]. A very representative spectrum of a calcium-rich glaze was recorded on the white area inside a black spot of iron-rich defects (spectrum h in Figure 8).

We observe a third characteristic signature exhibiting a doublet at ~980 and 1040 cm^{-1} (Figure 8-left e,f) associated with the characteristic peak of the As-O bond at ~815–820 cm^{-1} [25,26]. The As_2O_3 content can be measured up to 10 wt% with a small amount of PbO (up to 10 wt%) and about 2 wt% of Na_2O (Table 3). The ~980–1040 cm^{-1} SiO_4 stretching doublet is similar with the signature of an Iznik glaze (Iznik fritware is the most characteristic Ottoman pottery dating to the 15th–17th centuries), with a similar sodium-and-lead-based flux [53]. A significant amount of PbO was detected in the gilded area (~10–25 wt%, Figure 7-right and Figure 9-right).

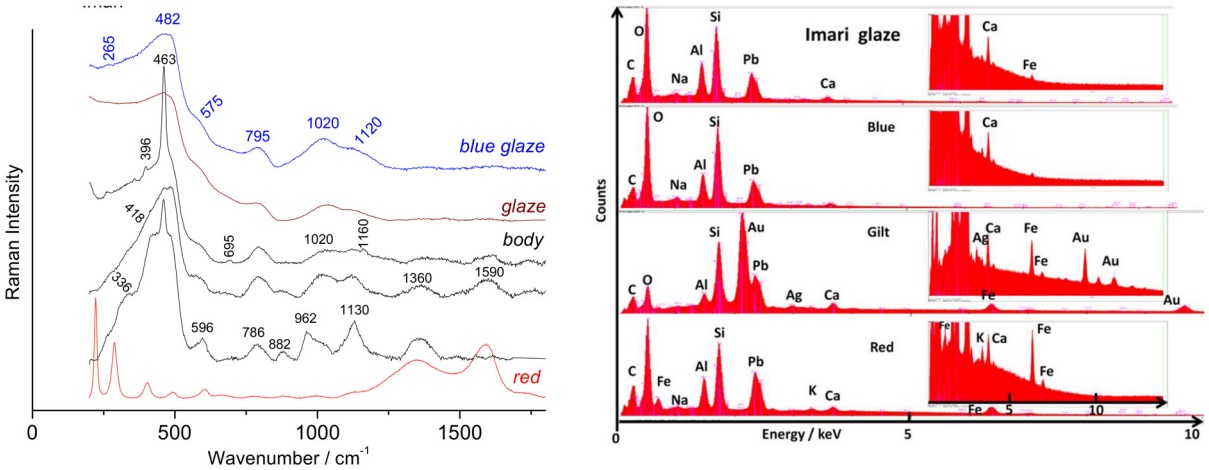

Figure 9. Representative Raman spectra (**left**) and EDXS spectra (**right**) recorded on Imari-style Chinese plate (Figure 2f): blue and colorless glaze surface, body section and red area paint.

The enameled decoration of the plate representing a rose (Rose plate, Appendix A, Figure A1e) offers a large set of enamels of various colors (and techniques as we will see). We will analyze them in detail. An additional broad band at ~1280 cm^{-1} is observed in some spots (Figure 10-right and Figure A1e). The intensity of the ~1280 cm^{-1} band is very variable when the analyzed spot is displaced across the blue colored area.

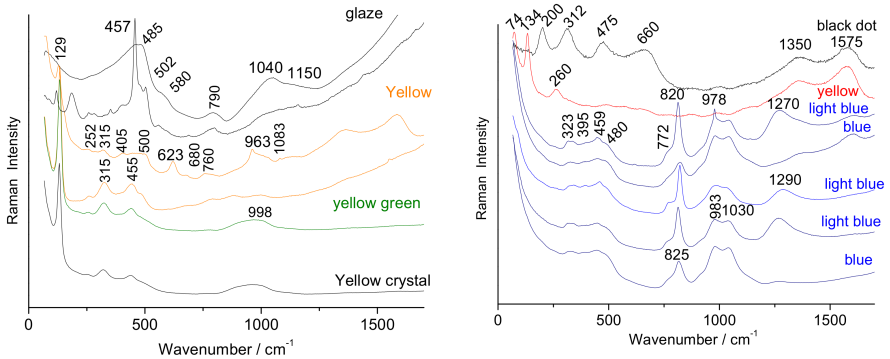

Figure 10. Representative Raman spectra recorded on section (**left**) and surface (**right**) on Rose plate (Figures 3 and A1e).

Additionally, the band is barely visible using green laser excitation. Such a signature is unusual but has already been observed in the study of blue overglazed soft-paste porcelains [72] produced at Sèvres Royal Factory in 1781 [80]. Bands in this spectral range are rare and characteristic of the B-O_3 stretching mode [81–84] that indicates the use of borax in the formulation of the enamel. Boron is very volatile (i.e., a large amount disappears during the firing) and not detected by most of the techniques used to measure elemental composition. The amount of boron kept in the glaze is thus lower than the initial content in the glaze precursor.

Maggetti and d'Albis failed to detect boron in this enamel by XRF but reported that borax had been used for the preparation of the blue enamel [80], citing the previous book of Préaud and d'Albis [85], which reports *Hellot*'s color recipes written in 1753 in many manuscripts kept in the archives of the Manufacture Nationale de Sèvres [86]. *Jean Hellot* (1685–1766) made seminal contributions to the development of the chemical and metallurgical processes, such as ceramic and textile industry in France and beyond [87,88]. He was appointed by the King of France in June 1751 to get hold of the secrets of the porcelain production which were, until then, scattered among different hands, in order that the future Royal Porcelain Factory of Sèvres had the best know-how. Summaries of these manuscripts have been published [85,89–93].

A new type of Raman signature is observed for the Imari-style plate (Figure 9). The strong broad band peak at 482 cm^{-1} is present and the doublet component at 1020 cm^{-1} is stronger than that of the second one at ~1120 cm^{-1}. EDXS analysis indicates the presence of lead. However, the amount is small, likely between 10 and 30 wt% (see representative local composition listed in Table 2).

The Raman signature of a glassy silicate network of glazes and enamels is now well-understood [75–79]. The Raman spectrum of a glaze consists of two broad 'bands', at about 450–500 and 900–1100 cm^{-1}, arising from the bending and stretching modes of the SiO_4 tetrahedron which is the basic unit of silicates, either crystalline or amorphous. However, due to the large deformation of the Si-O bond in a symmetrical bending mode (at ~450–500 cm^{-1}), this mode dominates the Raman spectrum of a highly connected Si-O network. On the contrary, the intensity of the second band (SiO_4 symmetric stretching mode) increases with the depolymerization and is maximal for an isolated SiO_4 tetrahedron [75–79]. A direct link was established between the spectral components of the stretching band and the different more or less connected SiO_4 tetrahedrons. The less the Si-O bonds are connected, the lower the wavenumber of the stretching mode will be. Thus, the center of gravity of the stretching bands is correlated to the melting temperature of a silicate [75–79]. The relative intensity of the bending mode area versus the stretching mode also characterizes the degree of polymerization and hence the melting temperature. The intensity of the stretching modes is thus very low for an (aluminum/silicon-rich) glaze fired at a high temperature (>1200 °C, e.g., Na-K glaze). On the contrary, glass that melts at a low temperature (<900 °C, e.g., lead-rich or flux-rich enamel) shows bands in the 900–1000 cm^{-1} range with a stronger intensity [75–79].

The characteristic Raman signatures of opacifiers (cassiterite, arsenic-rich phases) and pigments (hematite (red), lead stannate/antimonate (Naples yellow pyrochlore group), iron/manganese–based spinels (black)) have been well-documented previously by many studies of 18th century Chinese, Japanese or European artefacts [22–26,28,31–35,94–105]. Signatures of the characteristic enamels colored using gold metal nanoparticles are also known [32–35]. We should recall that the Raman spectrum of a glass colored by ions dissolved in the glassy network (Cu^{2+} for green to turquoise hue, Co^{2+} for blue), does not exhibit specific features.

Both the Raman signature of the common K-Na-based glaze with a characteristic low-intensity 1030–1150 cm^{-1} doublet and the SiO_4 stretching mode peaking at 1040 cm^{-1} characteristic of a lead-(earth)alkali glaze are observed (Figure 10) [76]. The latter glaze signature is comparable to that of the Imari-style plate (Table 2 and Figure 9) and is characteristic of the contamination with lead or its addition.

The spectra of flowers with pink and blue petals shown in Figure 3 (Rose plate, Figure A1e) are interesting. The blue enamel everywhere shows the peak at ~820 cm^{-1} characteristic of As-apatite [106] and a SiO_4 stretching band characteristic of lead-alkali enamel (doublet~980–1030 cm^{-1}). In the periphery (light blue), the additional Raman signature (1260 to 1290 cm^{-1}) of the triangular BO_3 species indicates the use of borax according to the recipe given by *Hellot* [85,91]. The black point shows the spectrum of the dendritic epsilon-Fe_2O_3 phase, commonly observed in the presence of a local excess of flux [55,94,95]. Several kinds of Naples yellow pyrochlore phases with the main peak at 129 or 134 cm^{-1} are observed according to the shade of yellow. Observation of the pure $Pb_2Sn_2O_6$ spectrum (~130, 315 and 455 cm^{-1}) [22,24,29–32,34,96–105] with a 100× objective indicates grains of a few microns in size, consistent with the use of a pre-prepared pigment and not nucleation-precipitation by saturation with lead and tin. Some wollastonite is however detected (623–963 cm^{-1} doublet) [52,55] in relation with the high level of CaO. The colors yellow to green are lead enamels as for the blue, but without borax. There is good agreement between the EDXS (Table 3) and Raman measurements (Figure 10).

3.3. Non-Invasive Analysis of Rare Objects

Pronk' coffee pot (Figure 11a).

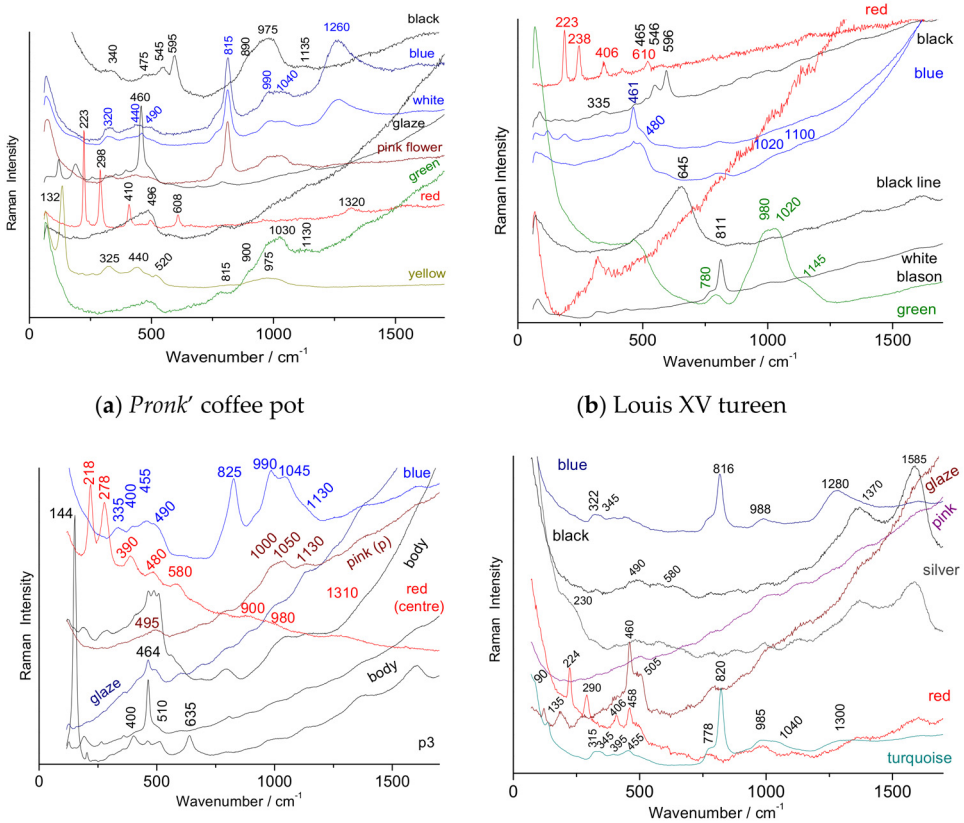

(**a**) *Pronk*' coffee pot (**b**) Louis XV tureen

(**c**) *Orry* dish (**d**) *La Bistrate & Proli* dish

Figure 11. Representative Raman spectra recorded on different colored areas of the *Pronk* coffee pot (**a**), the tureen with the royal coat-of-arms of France (**b**), the *Orry* armorial dish (**c**) and the plate with the arms of the *la Bistrate*-and-*Proli* Family (**d**).

The Raman spectrum of the colorless glaze is characteristic of a K-Na glaze. The red color was obtained with hematite (peaks at 223, 298, 410, 496, 608 and 1320 cm^{-1}, Figure 10-left) [32–34,107].

The very narrow hematite peaks indicate a pure α–Fe_2O_3 phase [107]. The yellow color was obtained with the use of a $Pb_2Sn_2O_6$ type pigment with characteristic peaks

at 132, 325 and 440 cm^{-1} [32–34,96–104]. A black line spectrum exhibits the bands characteristic of a Mn-rich spinel at ~600 cm^{-1} [94,95], plus a strong ~975 cm^{-1} band characteristic of a depolymerized silicate molten at low temperature [74–77] obtained by the addition of PbO. White and blue areas show the signature of arsenic apatite with a complex formula $Na_{1-x-2y}K_xCa_yPb_4(AsO_4)_3$ (strong 815, 790 shoulder, weaker 440 and 320 cm^{-1} bands [26,28,72,106]) associated with the SiO_4 stretching mode doublet at 990 and 1040 cm^{-1} as well as the ~1260 cm^{-1} B–O_3 band observed on an Imari-style plate due to the use of borax. Green areas show a Raman spectrum intermediate between those of the glaze and the black enamel that indicate a strong reaction between the glaze and the green overglaze.

Tureen with Louis XV Royal coat-of-arms (Figure 11b)

The spectra recorded on the tureen of the Louis XV set indicate the deposition of low-temperature enamels (strong 980 cm^{-1} peak) on a standard K-Na glaze (small intensity 1020–1100 cm^{-1} doublet). The red pigment is similar with that of the *Pronk* coffee pot, namely well-crystallized α–Fe_2O_3 hematite. The broad band of the black line corresponds to a disordered Fe-based spinel (broad 645 cm^{-1} peak). A black pigment with another composition, probably Mn-rich, was observed in the black areas (596 cm^{-1} peak). The white enamel exhibits a strong and narrow 811 cm^{-1} peak characteristic of arsenic apatite [26,28,72,106]. Due to the high level of opacifier in the white enamel, it is not possible to characterize the enamel matrix.

Orry armorial dish (Figure 11c).

Spectra recorded from the *Orry* armorial dish are different. Firstly, the porcelain body exhibits the signature of anatase (144, 400 and 635 cm^{-1} peaks), a common impurity of kaolin. This can also be the proof of pollution due to previous restoration work (to hide certain cracks or gaps). As expected, the signatures of quartz (464 cm^{-1}), feldspar/plagioclases (510 cm^{-1}) and cristobalite (400 cm^{-1}) [72] were also detected.

The blue overglaze shows a strong As-O band, but broad and peaking at 825 cm^{-1}. This has been previously observed for Chinese porcelain [26,32,95,105] and associated with the use of cobalt ore imported from Europe. The shift and broadening of the peak are assigned to the formation of a phase with a structure different from apatite (likely As-based feldspar, see discussion in ref. [95]) and/or to the nucleation of the As-rich phase in the form of disordered nanoparticles. The bandwidths of the Raman bands of hematite are also broad, indicating a partial substitution of Fe ions with Ti or Al [107].

The spectrum recorded on the pink area shows the characteristic spectrum of a glassy silicate with a medium intensity of the 495 and ~1000 cm^{-1} bands. The absence of peaks characteristic of any pigment is consistent with coloration by metal nanoparticles (copper or gold, it is not possible to distinguish between them by Raman spectroscopy) [32,34,35,105], but the quality of the spectrum recorded indicates that some areas (at the micron scale, the size of the area analyzed by the Raman microscope) are free or contain a low amount of metal nanoparticles as observed in sampled plates.

La Bistrate-and-Poli' Family dish (Figure 11d).

The Raman signature of the glaze corresponds to standard Na-K glaze fired with the porcelain body with additional components of quartz (460 cm^{-1}) and feldspar/plagioclase (505 cm^{-1}). The signature from the red areas is that of pure, well-crystallized hematite (see above), but mixed with quartz. The turquoise and blue enamels exhibit a strong arsenic-based apatite signature (820 cm^{-1} narrow peak with a 780 cm^{-1} shoulder [72,106]), but the silicate matrices are different for the two colors: a single SiO_4 stretching band at ~988 cm^{-1} is observed for the blue in accord with the large addition of PbO, but a 985–1040 cm^{-1} doublet is observed for the turquoise area, indicating a more polymerized glassy matrix, fired at a higher temperature. Furthermore, the spectrum of the blue enamel exhibits a strong and broad 1280 cm^{-1} peak characteristic of the use of borax. The pink area shows a weak Raman spectrum superimposed on intense fluorescence, as expected for a pink color obtained with gold nanoparticles [34].

A very specific color in the plate is the silvering decoration. Its spectrum shows broad bands at 480 and 230 cm^{-1} plus the 1370–1585 cm^{-1} doublet characteristic of carbon. The

230 cm^{-1} band is consistent with silver sulfide [108,109], the common corrosion film formed on silver.

The broadening of the band is consistent with the presence of nanoparticles and/or a high disorder. A strong carbon doublet is very commonly observed on metal films due to the Surface Enhancement Raman Scattering effect (SERS). The carbon doublet was also recorded on the black lines as well as a broad band at 580 cm^{-1} consistent with a spinel pigment.

Duc de Penthièvre plate (Figure 12a).

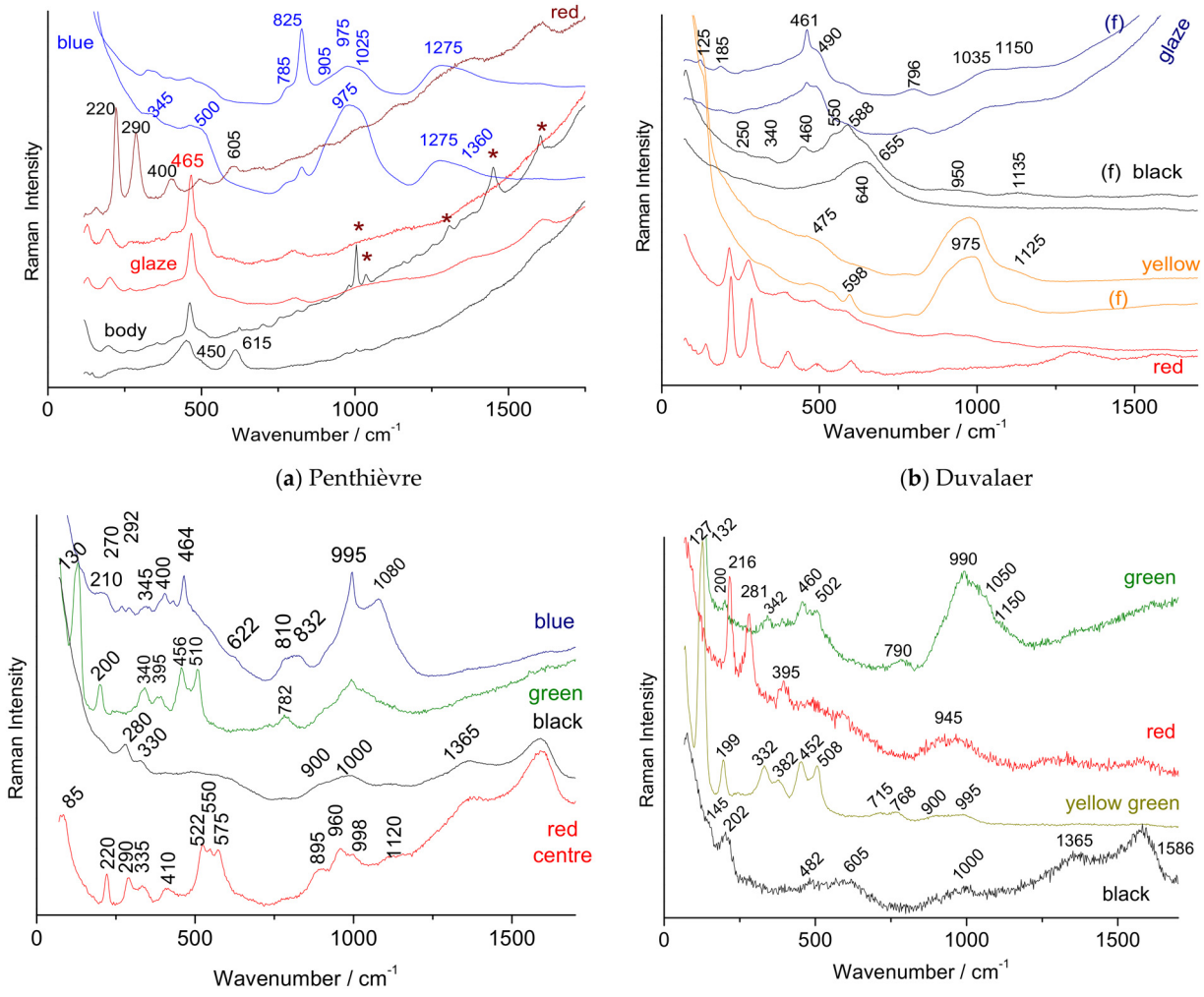

Figure 12. Representative Raman spectra recorded on different colored areas of the dish with the coat-of-arms of the *Duc de Penthièvre* (**a**), an ewer with the coat-of-arms of the *Duvalaer* family (**b**) and (**c**) of the Dutch-decorated plate.

The body and glaze seem to be richer in un-dissolved quartz grains. Indeed, the signature of quartz is commonly observed as shown in Figure 12a. The standard signature of a K-Na glaze is observed in this plate. The peaks of the spectrum of hematite (red areas) are rather narrow but larger than those which were observed for the *Pronk*' coffee pot, Louis XV tureen, and the *la Bistrate*-and-*Poli* plate. The blue areas show different Raman signatures where in some places the narrow and strong peak characteristic of an arsenic-based apatite was detected, but observed at 825 cm^{-1}.

In other places, its intensity is lower. The signature of the silicate matrix shows strong broad bands at 975 and 1275 cm^{-1} consistent with the addition of PbO and borax. Rutile

was detected (450–615 cm^{-1} doublet) [110] in the body. It could be intrinsic (TiO_2 rutile is a very good Raman scatterer and is a minor phase associated with many tecto- and phyllosilicates) or a pollutant arising from cleaning and minor restoration treatment.

Duvelaer ewer (Figure 12b).

The glaze exhibits the standard Raman spectrum of a K-Na glaze. Specific spectra were observed for the yellow enamels, with some differences noted between the foot and the upper part of the ewer. For both regions, the SiO_4 stretching mode peak at 975 cm^{-1} is observed (lead-based overglaze). Additional small peaks at 125 cm^{-1} ($Pb_2Sn_2O_6$ pigment) [22,24,32,34,96–105] and 598 cm^{-1} (trace of red spinel or hercynite?) are also observed for the yellow enamel at the foot. Two types of red hematite were identified, one with narrow peaks, the other with broader ones, in accord with a partial substitution of Fe ions by Al or Ti ones. Two different signatures were also observed for the black lines, corresponding to more or less disordered spinels of different composition.

Dutch-decorated plate (Figure 12c).

This plate shows a variety of spectra which are rather different from those recorded on Chinese porcelains, in confirmation with the application of the decoration in the Low-Countries. The center of gravity of the SiO_4 stretching band is at about 975 cm^{-1} as for the Chinese lead-based overglazes (the processing temperature should be rather similar), but the shape is different. A strong narrow peak at ~995 cm^{-1} characteristic of pseudo-wollastonite (β–$CaSiO_3$, additional peaks at ~375, 580, 625 and 1075 cm^{-1}) [52,55,72] indicates the saturation of the glaze with calcium as observed for the yellow overglaze of the Rose plate (Figure 10). The signature of the complex pyrochlore composition was detected for the green and yellow-green enamels (peaks at 130, 200, 340, 395 and 510 cm^{-1}) [34,96–105]. This type of Naples yellow pigment is not generally observed in Chinese enameled decoration before the Qianlong period [32,105], i.e., about a decade after the expected date of the production of this plate. Specific spectra were also observed for the black and red enamels.

4. Discussion

Table 4 summarizes the main conclusions regarding the identification of phases used as pigment or opacifier. As previously observed, two types of colorless glaze were identified, Ca-rich (wollastonite can even be detected indicating a saturation with calcium) and standard Na-K-Ca-based glaze. Except for Louis XV tureen in which blue color was put under/in-glaze (cannot be attested without examining a fracture), all other blue colored (overglaze) areas of the analyzed masterpieces contain arsenic. This is consistent with the use of European cobalt.

For the first time, the use of borax in the blue overglaze of artefacts made in 1735–1740 according to the recipe from the 1753-manuscripts of the chemist *Hellot* is demonstrated on Chinese enameled porcelain. Detection of borate glass obtained at the periphery of the blue colored area seems to be only easy with the blue laser line. This is consistent with the low viscosity of the boron-based glass and indicates certain heterogeneity of the glassy blue enamel. The dates established according to the stylistic analysis and the historical data indicate the use of borax-based enamel in China, long before the realization of an inventory of enameling recipes by *Hellot* in 1753. It is logical to think that the recipes collected to compile this state-of-the-art report were already well-established and dated back several years earlier. However, the first multicolored decorations on porcelain were not common until the 1730s Meissen productions [10,11]. The time gap between the use of new enameling recipes in Europe and in Chinese workshops working for export is therefore small. On the contrary, the Louis XV tureen uses classic Chinese techniques (blue underglaze or in-glaze characteristic of *Famille verte* porcelain). Arsenic-based apatite is used to make the white enamel in all artefacts except the older one, the *Duvelaer* ewer (circa 1720–1725, Table 1).

Table 4. Summary of the main technical characteristics identified by on-site non-invasive Raman scattering. Characteristic Raman peak wavenumbers are given.

Artefact	Period	Body	Glaze (cm^{-1})								
			Colourless	**Blue**	**White**	**Green**	**Red**	**Pink**	**Black**	**Yellow**	**Siver**
Dutch decorated dish	1710–1730		975 (Ca-based) Wollastonite (995)	No As Wollastonite (995)		Complex NY (130,510)	Hematite + other phase (522–575)			Complex NY (130, 510)	
Duvelaer ewer	1720–1725		K-Na (1035–1150)				2 types of hematite (road & narrow) + NY		2 spinel phases (588 & 640)	(975) NY (125) (598 spinel?)	
Philibert Orry' dish	circa 1730	Feldspar Quartz anatase	(1050) K-Na	As (820, broad)			Hematite (broad)	(1000–1050)	(975) Spinel (595)		
La Bistrate and *Poli* dish	1730–1735		K-Na (1035–1150)	As-apatite (816) Borax			Hematite (narrow)				(230) Ag_2S
Duc de Penthièvre dish	circa 1737		K-Na	As-apatite (825) Borax (1275)			Hematite (medium)		carbon		
Louis XV tureen	circa 1738			(1020–1100) underglaze	As-apatite (811)	(980–1020)	Hematite (narrow)		Spinel (595) Spinel (645,)		
Pronk coffee pot	1730–1740		quartz	As-apatite (815) Borax (1260)	As-apatite (815)	(975–1030) As (815)	Hematite (narrow)	As-apatite (815)	Spinel (595 (975))	$Pb_2Sn_2O_6$ (132)	

Contemporary productions using 'classical' Chinese techniques and others preferentially using imported techniques are likely. Our analyses have shown that if the use of imported recipes started at the end of the reign of Emperor Kangxi [25,105], circa 1716, see below, then there was a return to traditional techniques under the Yongzheng reign. Indeed, imperial workshops were established at the Forbidden City in Beijing to satisfy the demand of Kangxi Emperor that 'new' objects similar with those given as presents by the Jesuits and Emissary of Louis XIV could be locally produced. The first imperial workshop opened in 1693 to manufacture *cloisonné* enamels. It is assumed that preparation of painted enamels had started with the opening of a glass workshop in 1696. A dedicated enameling workshop then opened in 1716 [13,16,17,35]. At the same time, or before, another production center of painted enamels was established in Guanzhou (Custom district). It is known that the Jesuits lost their influence under the reign of Yongzheng and one can think that this was reflected in the technical practices that they had introduced. However, according to the workshops (Beijing, Jingdezhen or Canton), imperial or private, the modification practices could also vary. The highlighting of the use of different recipes or raw materials for porcelain from the same period can therefore be the signature of different workshops. Thus, three different Raman signatures are identified by the width of the hematite vibration modes: very narrow modes for *Pronk*' coffee pot and Louis XV tureen, broad for *Orry*' dish and intermediate for the others. At least three different workshops are thus expected. A priori, all these ceramics being of high quality, we can exclude a choice of ingredients only imposed by the cost of raw materials. Many of these hypotheses need to be verified by examining a larger number of artefacts. The selection criterion by the color is also to be taken into account since for the *Duvelaer* ewer, two types of hematites were used. It is the same for the realization of the black color, and the yellow and green colors with at least three techniques used for black (two different spinels and carbon) as well as for yellow-green (three different Naples yellow pyrochlores, tin-rich, antimony-substituted and fired at different temperatures). The dish with the coat-of-arms of the la *Bistrate & Poli* families is decorated with silver plating recognized by its color and the detection of its surface corrosion with silver sulfide. This technique can also be specific to a workshop.

It is interesting to note that the use of arsenic for the realization of the white overglaze corresponds to the latest objects, made after 1738. By comparison, arsenic-based phases were identified in many blue overglazes of artefacts made at the end of the Kangxi reign at the Palace workshop (i.e., before 1723 [25,105] while the use of arsenic-apatite was identified in only one artifact, a water dropper assigned to be produced at Jingdezhen [25]. This suggests that the innovation was not made only at the Palace workshop but also at the imperial kilns of Jingdezhen. Objects using voluntary arsenic opacification (i.e., identified in white overglaze) are attributed to productions after 1730, probably in private workshops, without the attribution making it possible to distinguish the private workshops of Jingdezhen or Canton (Guangzhou).

From the moment when the Chinese enamellers understood that obtaining nicer blue shades with the smalt imported from Europe as a source of cobalt came from its richness in arsenic, the detection of arsenic in the blue enamel can no longer be a direct proof of the use of smalt. Analysis of the microstructure, in particular by Transmission Electron (TEM) or Electron Back Scattering Scanning Electron Microscopy (EBS-SEM) is necessary.

5. Conclusions

This work clearly illustrates the wealth of information obtained by non-invasive Raman analysis. In the lack of joint XRF measurement, a good-knowledge of the Raman signatures obtained on similar samples also analyzed by SEM-EDXS appears to be sufficient for an unequivocal identification of most of the phases constituting the glaze and the enamels. Even a comparison of a limited number of pieces, but with sophisticated decor, provides sufficient information to discuss possible common places of production. A greater number of non-invasive analyses on exceptional pieces but also destructive analyses on rather similar artefacts of lower value should lead to a fair view of the dynamics of the

importation of European recipes (and ingredients) and their assimilation/development by Chinese artisans. Therefore, in the 18th century, China was both an importer of European know-how, design and a production workshop for the export of products made with imported technologies to Europe. The similarity with the present situation is disturbing, especially since in both periods maritime transport is a determining factor in the economic validation.

Author Contributions: Conceptualization, P.C.; methodology, P.C.; investigation, P.C. and A.-T.N.; resources, N.F.; writing—original draft preparation, P.C.; writing—review and editing, P.C., A.-T.N. and N.F. All authors have read and agreed to the published version of the manuscript.

Funding: This research received no external funding.

Institutional Review Board Statement: Not applicable.

Informed Consent Statement: Not applicable

Data Availability Statement: All data given in the text and Appendix A.

Acknowledgments: J.-B. Clais (Department of Fine Art objects, Louvre Museum, Paris) is kindly acknowledged for many discussions.

Conflicts of Interest: The authors declare no conflict of interest.

Appendix A

Figure A1. Plates: (**a**) BW f; (**b**) BW ww; (**c**) LA (**c'**) detail view); (**d**) PEO; (**e**) Rose. See Table 1 for more information.

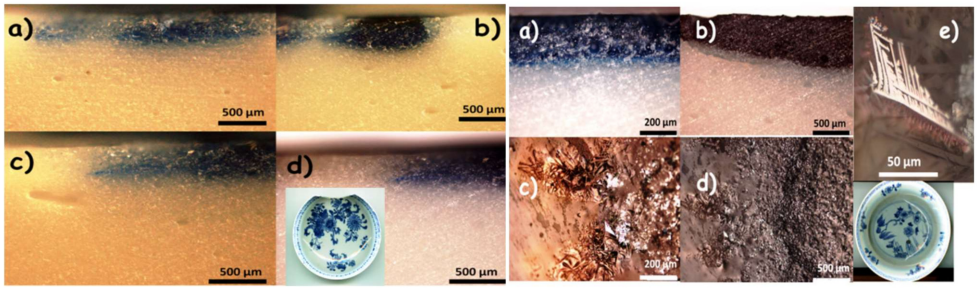

Figure A2. Section view of BW f plate (**left**, **a**–**d**) different sections) and BW ww (**right**, **a**) section and upper view of blue décor; (**b**) section of black defect spot; (**c**,**d**) surface view of the defect periphery; (**e**) dendrites.

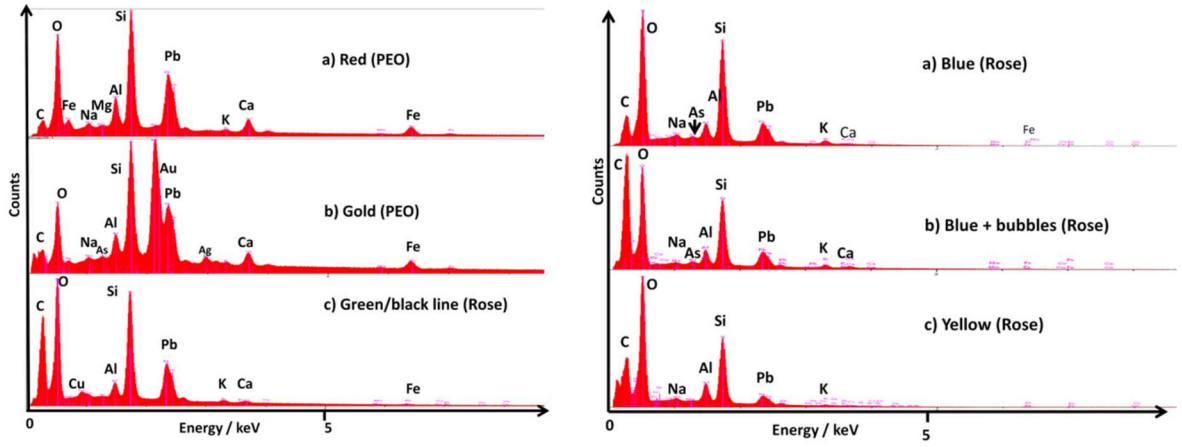

Figure A3. Representative EDXS spectra recorded on **left**, red (**a**) and gold (**b**) areas of PEO plate overglaze (50×), (**c**) green and black line of Rose plate; on **right**, on blue (**a**,**b**) smooth and bubble-rich blue petal and (**c**) yellow dot (see Figure 3a).

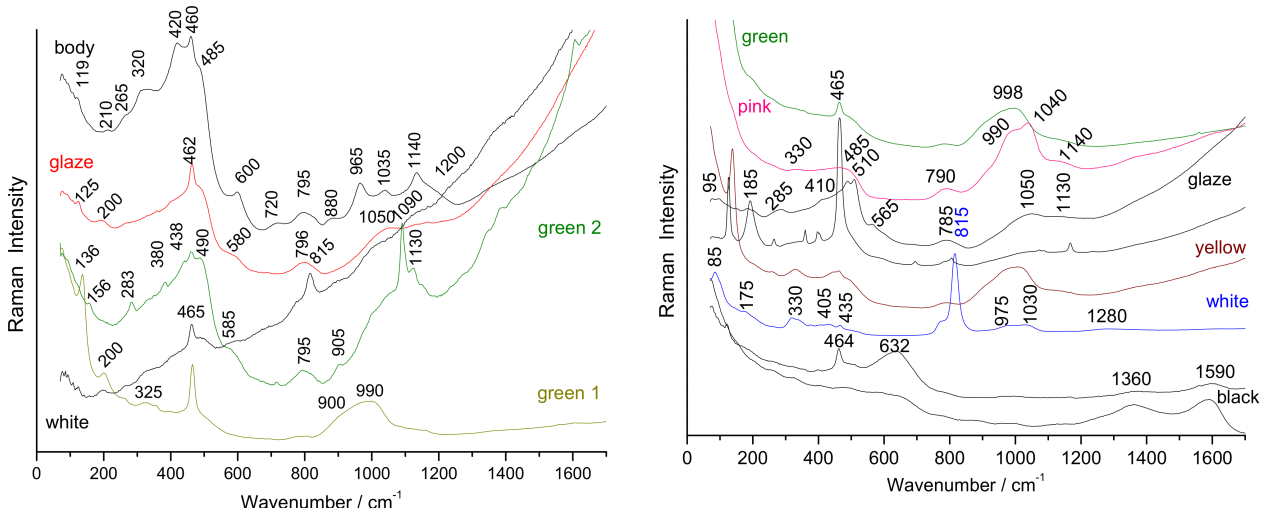

Figure A4. Representative Raman spectra recorded on PEO section (**left**) and surface (**right**).

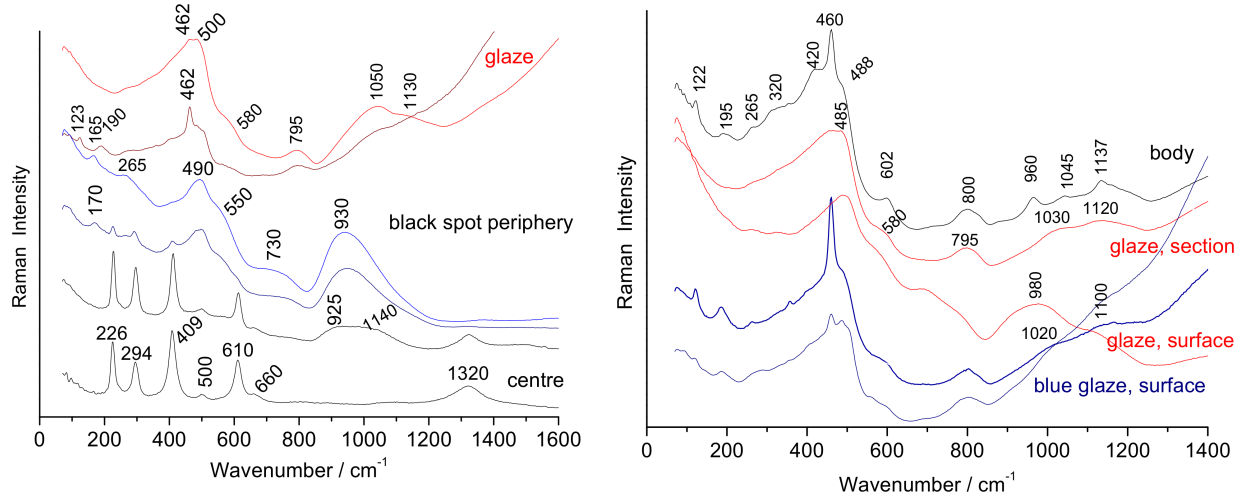

Figure A5. Representative Raman spectra recorded on BW ww (**left**) and BW f (**right**).

References

1. d'Entrecolle, F.-X. *Letters from Ching-Te-Chen in 1712 and 1722*; New York State Institute for Glaze Research: Painted Post, NY, USA, 1983.
2. Vogt, G. La porcelaine Chinoise. *Bull. Soc. d'Encouragement pour l'Industrie Nationale* **1900**, *99*, 530–612.
3. Levy, E. Le Goût Chinois en Europe au XVIIIe Siècle: Catalogue du Musée des Arts Décoratifs, June–October 1910, Librairie Centrale des Beaux-Arts Paris 1910. Available online: https://gallica.bnf.fr/ark:/12148/bpt6k441547m/f1.texteImage (accessed on 28 November 2021).
4. Lion-Goldschmidt, D. Les porcelaines chinoises du palais de Santos. *Arts Asiatiques* **1984**, *39*, 5–72. Available online: https://www.persee.fr/doc/arasi_0004-3958_1984_num_39_1_1616 (accessed on 28 November 2021). [CrossRef]
5. Ayers, J.; Impey, O.; Mallet, J.V.G. *Porcelain for Palaces: The Fashion for Japan in Europe 1650–1750*; Oriental Ceramic Society: London, UK, 1990.
6. Impey, O. Collecting Oriental Porcelain in Britain in the Seventeenth and Eighteenth Centuries. In *The Burghley Porcelains, an Exhibition from the Burghley House Collection and Based on the 1688 Inventory and 1690 Devonshire Schedule*; Japan Society: New York, NY, USA; Tokyo, Japan, 1990; pp. 36–43.
7. Alayrac-Fielding, V. From the curious to the "artinatural": The meaning of oriental porcelain in 17th and 18th-century English interiors. *Miranda* **2012**, *7*, 1–21. [CrossRef]
8. Castelluccio, S. *Le Gout pour les Porcelaines de Chine et du Japon à Paris aux XVIIe et XVIIIe Siècles*; Monelle Hayot Editions: Saint-Rémy-en-l'Eau, France, 2013.
9. van Campen, J.; Eliëns, T.M. *Chinese and Japanese Porcelain for the Dutch Golden Age*; Zwolle: Waanders Uitgevers, The Netherlands, 2014.
10. Faÿ-Hallé, A.; Lahaussois, C. *La Porcelaine Française au XVIIIe Siècle, Histoire, Motifs et Marques*; Les Essentiels du Patrimoine-Massin: Paris, France, 2011.
11. de Plinval de Guillebon, R. L'Eveil de la porcelaine à Paris. *Rev. Soc. Amis Musée National de Céramique*. 2005, pp. 55–68. Available online: http://www.amisdesevres.com/wp-content/uploads/2011/01/revue_19_55-68.pdf (accessed on 28 November 2021).
12. Edwards, H.G.M. *Porcelain Analysis and Its Role in the Forensic Attribution of Ceramic Specimens*; Springer: Cham, Switzerland, 2021. [CrossRef]
13. Shih, C.F. Evidence of East-West exchange in the eighteenth century: The establishment of painted enamel art at the Qing Court in the reign of Emperor Kangxi. *Natl. Palace Mus. Res. Q.* **2007**, *24*, 45–94.
14. Zhou, S.Z. *Research on Painted Enamels Porcelain Ware from the Qing Court*; Wenwu Chubanshe: Beijing, China, 2008.
15. Curtis, E. *Glass Exchange between Europe and China, 1550–1800*; Ashgate: Farnham, UK, 2009.
16. Lili, F. *La Céramique Chinoise*; China Intercontinental Press: Beijing, China, 2011.
17. Shih, C.F. *Radiant Luminance: The Painted Enamelware of the Qing Imperial Court*; The National Palace Museum of Taipei: Taipei, Taiwan, 2012.
18. Xu, X.D. Europe-China-Europe: The Transmission of the Craft of Painted Enamel in the Seventeenth and Eighteenth Centuries. In *Goods from the East, 1600–1800 Trading Eurasia*; Berg, M., Ed.; Palgrave Macmillan: London, UK, 2015; pp. 92–106.
19. Zhang, F. The origin and development of traditional Chinese glazes and decorative ceramic colors. In *Technology to Modern Science*; Kingery, W.D., Ed.; Ceramics and Civilization Series; The American Ceramic Society: Colombus, OH, USA, 1985; Volume 1, pp. 163–180.
20. Kingery, W.D.; Vandiver, P.B. The Eighteenth-Century Change in Technology and Style from the *Famille-Verte* Palette to the *Famille-Rose* Palette. In *Technology and Style*; Kingery, W.D., Ed.; Ceramics and Civilization Series; The American Ceramic Society: Colombus, OH, USA, 1986; Volume 2, pp. 363–381.
21. Wood, N. *Chinese Glazes: Their Origins, Chemistry and Recreation*; A & C Black: London, UK, 1999.
22. Kırmızı, B.; Colomban, P.H.; Quette, B. On-site analysis of Chinese *Cloisonné* enamels from fifteenth to nineteenth centuries. *J. Raman Spectrosc.* **2010**, *41*, 780–790.
23. Van Pevenage, J.; Lauwers, D.; Herremans, D.; Verhaeven, E.; Vekemans, B.; De Clercq, W.; Vincze, L.; Moens, L.; Vandenabeele, P. A Combined Spectroscopic Study on Chinese Porcelain Containing Ruan-Cai Colours. *Anal. Methods* **2014**, *6*, 387–394. [CrossRef]
24. Colomban, P.; Arberet, L.; Kırmızı, B. On-Site Raman Analysis of 17th and 18th Century Limoges Enamels: Implications on the European Cobalt Sources and the Technological Relationship between Limoges and Chinese Enamels. *Ceram. Int.* **2017**, *43*, 10158–10165. [CrossRef]
25. Colomban, P.; Zhang, Y.; Zhao, B. Non-invasive Raman analyses of huafalang and related porcelain wares. Searching for evidence for innovative pigment technologies. *Ceram. Int.* **2017**, *43*, 12079–12088. [CrossRef]
26. Colomban, P.; Ambrosi, F.; Ngo, A.-T.; Lu, T.-A.; Feng, X.-L.; Chen, S.; Choi, C.-L. Comparative analysis of wucai Chinese porcelains using mobile and fixed Raman microspectrometers. *Ceram. Int.* **2017**, *43*, 14244–14256. [CrossRef]
27. Giannini, R.; Freestone, I.; Shortland, A. European cobalt sources identified in the production of Chinese *Famille rose* porcelain. *J. Archaeol. Sci.* **2017**, *80*, 27–36. [CrossRef]
28. Colomban, P.; Lu, T.-A.; Milande, V. Non-invasive on-site Raman study of blue-decorated early soft-paste porcelain: The use of arsenic-rich (European) cobalt ores—Comparison with huafalang Chinese porcelains. *Ceram. Int.* **2018**, *44*, 9018–9026. [CrossRef]

29. Montanari, R.; Alberghina, M.F.; Casanova Municchia, A.; Massa, E.; Pelagotti, A.; Pelosi, C.; Schiavone, S.; Sodo, A. A polychrome Mukozuke (1624–1644) porcelain offers a new hypothesis on the introduction of European enameling technology in Japan. *J. Cult. Herit.* **2018**, *32*, 232–237. [CrossRef]
30. Montanari, R.; Murakami, N.; Alberghina, M.F.; Pelosi, C.; Schiavone, S. The Origin of overglaze-blue enameling in Japan: New discoveries and a reassessment. *J. Cult. Herit.* **2019**, *37*, 94–102. [CrossRef]
31. Montanari, R.; Murakami, N.; Colomban, P.; Alberghina, M.F.; Pelosi, C.; Schiavone, S. European Ceramic technology in the Far East: Enamels and pigments in Japanese art from the 16th to the 20th century and their reverse influence on China. *Herit. Sci.* **2020**, *8*, 48. [CrossRef]
32. Colomban, P.; Kırmızı, B.; Zhao, B.; Clais, J.-B.; Yang, Y.; Droguet, V. Non-invasive on-site Raman study of pigments and glassy matrix of the 17th–18th century painted enamelled Chinese metal wares: Comparison with French enamelling technology. *Coatings* **2020**, *10*, 471. [CrossRef]
33. Colomban, P.; Kırmızı, B. Non-invasive on-site Raman study of polychrome and white enamelled glass artefacts in imitation of porcelain assigned to Bernard Perrot and his followers. *J. Raman Spectrosc.* **2020**, *51*, 133–146. [CrossRef]
34. Colomban, P.; Kırmızı, B.; Gougeon, C.; Gironda, M.; Cardinal, C. Pigments and glassy matrix of the 17th–18th century enamelled French watches: A non-invasive on-site Raman and pXRF study. *J. Cult. Herit.* **2020**, *44*, 1–14. [CrossRef]
35. Colomban, P.; Gironda, M.; Vangu, D.; Kırmızı, B.; Zhao, B.; Cochet, V. The technology transfer from Europe to China in the 17th–18th centuries: Non-invasive on-site XRF and Raman analyses of Chinese Qing Dynasty enameled masterpieces made using European ingredients/recipes. *Materials* **2021**, *14*, 7434. [CrossRef]
36. Howard, D. *Chinese Armorial Porcelain*; Faber & Faber: London, UK, 1952; Volume 1.
37. Jourdain, M.; Soame, J. *Chinese Export Art in the 18th Century*; Spring Books: Feltham, UK, 1967.
38. Le Corbeiller, C. China trade armorial porcelain in America. *Antiques* **1977**, *112*, 1124–1129.
39. Godden, G.A. *Oriental Export Market Porcelain and Its Influence on European Wares*; Grenada: London, UK; New York, NY, USA, 1979.
40. Le Corbeiller, C.; Frelinghuysen, A.C. Chinese Export Porcelain. *Metrop. Mus. Art Bull.* **2003**, *60*, 1–60. [CrossRef]
41. Howard, D.S. *Chinese Armorial Porcelain*; Heirlomm & Howard: London, UK, 2003; Volume 2, p. 155.
42. Lebel, A. *Armoiries Françaises et Suisses sur la Porcelaine de Chine au XVIIIe Siècle*; Antoine Lebel: Bruxelles, Belgium, 2009.
43. Castellucio, S. *Le Roi et la Compagnie Française des Indes Orientales, in La Chine à Versailles, Art et Diplomatie au XVIIIe Siècle*; De Rocherunne, M.L., Ed.; Somogy Editions d'Arts: Paris, France, 2014; pp. 94–119.
44. Un Cabinet Dédié aux Porcelaines. Available online: https://www.chateauversailles.fr/actualites/vie-domaine/cabinet-porcelaines#les-collections-presentees (accessed on 12 November 2021).
45. Sothebys. Available online: https://www.sothebys.com/en/auctions/ecatalogue/2008/the-collection-of-khalil-rizk-n08411/lot.4.html?locale=en (accessed on 12 November 2021).
46. Christies. A Chinese Export French Royal Ecuelle and Cover. Available online: https://www.christies.com/lot/lot-5648195 (accessed on 12 November 2021).
47. Christies. A Set of Three Graduated French Royal Armorial Ecuelles and Covers. Available online: https://www.christies.com/lot/lot-a-set-of-three-graduated-french-royal-6187630/?from=salesummary&intObjectID=6187630&lid=1 (accessed on 12 November 2021).
48. Christies. A Set of French Market Armorial Dishes. Available online: https://www.christies.com/en/lot/lot-6187628 (accessed on 12 November 2021).
49. Gotheborg Armorial Porcelain. Available online: https://gotheborg.com/glossary/armorial.shtml (accessed on 28 November 2021).
50. Colomban, P.; Treppoz, F. Identification and differentiation of ancient and modern European porcelains by Raman macro- and micro-spectroscopy. *J. Raman Spectrosc.* **2001**, *32*, 93–102. [CrossRef]
51. Colomban, P.; Sagon, G.; Faurel, X. Differentiation of antique ceramics from the Raman spectra of their coloured glazes and paintings. *J. Raman Spectrosc.* **2001**, *32*, 351–360. [CrossRef]
52. Colomban, P.; Robert, I.; Roche, C.; Sagon, G.; Milande, V. Identification des porcelaines "tendres" du 18ème siècle par spectroscopie Raman: Saint-Cloud, Chantilly, Mennecy et Vincennes/Sèvres. *Rev. d'Archéomètrie* **2004**, *28*, 153–167. Available online: https://www.persee.fr/doc/arsci_0399-1237_2004_num_28_1_1070 (accessed on 20 December 2021).
53. Colomban, P.; Milande, V.; Le Bihan, L. On-site Raman analysis of Iznik pottery glazes and pigments. *J. Raman Spectrosc.* **2004**, *35*, 527–535. [CrossRef]
54. Colomban, P.; Milande, V. On-site Raman analysis of the earliest known Meissen porcelain and stoneware. *J. Raman Spectrosc.* **2006**, *37*, 606–613. [CrossRef]
55. Colomban, P.; Ngo, A.-T.; Edwards, H.G.M.; Prinsloo, L.C.; Esterhuizen, L.V. Raman identification of the different glazing technologies of Blue-and-White Ming porcelains. *Ceram. Int.* **2021**, *48*, 1673–1681. [CrossRef]
56. Colomban, P.; Edwards, H.G.M.; Fountain, C. Raman spectroscopic and SEM/EDXS analyses of high translucent Nantgarw porcelain. *J. Eur. Ceram. Soc.* **2020**, *40*, 4664–4675. [CrossRef]
57. Neri, E.; Morvan, C.; Colomban, P.; Guerra, M.F. Late Roman and Byzantine mosaic opaque 'glass-ceramics' tessarae (5th–9th century). *Ceram. Int.* **2016**, *42*, 18859–18869. [CrossRef]
58. Christies. A Very Rare 'Pronk' Coffee-Pot and Cover. Available online: https://www.christies.com/en/lot/lot-5171857 (accessed on 12 November 2021).

59. Galerie Nicolas Fournery. Paire de Petits Plats Aux Armes de Philibert Orry, Contrôleur Général des Finances, en Porcelaine de Chine D'époque Yongzheng. Available online: https://www.galerienicolasfournery.fr/collection/paire-de-petits-plats-aux-armes-de-philibert-orry-de-vignory-controleur-general-des-finances-en-porcelaine-de-chine-depoque-yongzheng/ (accessed on 12 November 2021).
60. lot-5033522. Available online: https://www.christies.com/en/lot/lot-5033522 (accessed on 12 November 2021).
61. Musee Lorient. Available online: https://musee.lorient.bzh/collections/une-semaineune-oeuvre/bourdaloue/ (accessed on 12 November 2021).
62. Noblesse & Royautés. Vente d'un Plat de Service du Duc de Penthièvre. Available online: http://www.noblesseetroyautes.com/vente-dun-plat-de-service-du-duc-de-penthievre/ (accessed on 12 November 2021).
63. Galerie Nicolas Fournery. Assiette à Décor Armorié pour le Marché Belge (Bistrate d'Anvers) en Porcelaine de Chine D'époque Yongzheng. Available online: https://www.galerienicolasfournery.fr/collection/coupe-a-decor-armorie-pour-le-marche-hollandais-bistrate-danvers-en-porcelaine-de-chine-depoque-yongzheng/ (accessed on 12 November 2021).
64. Wikipedia. Cornelis Pronk. Available online: https://fr.wikipedia.org/wiki/Cornelis_Pronk (accessed on 12 November 2021).
65. Jörg, C.J.A. *Pronk Porcelain: Porcelain after Designs by Cornelis Pronk*; Groninger Museum: La Haye, The Netherlands, 1980.
66. Jörg, C.J.A. *Chinese Export Porcelain. Chine de Commande from the Royal Museum of Art and History in Brussels*; Urban Council: Hong Kong, China, 1989.
67. Lunsingh Scheurleer, D.F. *Chinese Export Porcelain-Chine de Commande*; Pitman Publishing Corporation: New York, NY, USA, 1974.
68. Howard, D.; Ayers, J. *China for The West Chinese Porcelain and Other Decorative Arts for Export Illustrated from the Mottahedeh Collection*; Sotheby Parke Benet: London, UK, 1978.
69. Kroes, J. *Chinese Armorial Porcelain for the Dutch Market*; Waanders BV: Uitgeverij, The Netherlands, 2007.
70. Krahl, R.; Harrison-Hall, J. *Chinese Ceramics—Highlights of the Sir Percival David Collection*; British Museum Press: London, UK, 2009.
71. Colomban, P.; Calligaro, T.; Vibert-Guigue, C.; Nguyen, Q.L.; Edwards, H.G.M. Dorures des céramiques et tesselles anciennes: Technologies et accrochage. *ArchéoSciences* **2005**, *29*, 7–20. [CrossRef]
72. Colomban, P.; Maggetti, M.; d'Albis, A. Non-invasive Raman identification of crystalline and glassy phases in a 1781 Sèvres Royal Factory soft paste porcelain plate. *J. Eur. Ceram. Soc.* **2018**, *38*, 5228–5233. [CrossRef]
73. Michel, D.; Colomban, P.; Abolhassani, S.; Voyron, F.; Kahn-Harari, A. Germanium mullite: Structure and vibrational spectra of gels, glasses and ceramics. *J. Eur. Ceram. Soc.* **1996**, *16*, 161–168. [CrossRef]
74. Colomban, P.; Paulsen, O. Non-destructive Raman Determination of the Structure and Composition of Glazes by Raman Spectroscopy. *J. Am. Ceram. Soc.* **2005**, *88*, 390–395. [CrossRef]
75. Colomban, P. Polymerization degree and Raman identification of ancient glasses used for jewellery, ceramic enamels and mosaics. *J. Non-Crystall. Solids* **2003**, *323*, 180–187. [CrossRef]
76. Colomban, P.; Tournié, A.; Bellot-Gurlet, L. Raman identification of glassy silicates used in ceramic, glass and jewellery: A tentative differentiation guide. *J. Raman Spectrosc.* **2006**, *37*, 841–852. [CrossRef]
77. Colomban, P. Non-destructive Raman analysis of ancient glasses and glazes. In *Modern Methods for Analysing Archaeological and Historical Glass*, 1st ed.; Janssens, K., Ed.; John Wiley & Sons: London, UK, 2012; pp. 275–300.
78. Labet, V.; Colomban, P. Vibrational properties of silicates: A cluster model able to reproduce the effect of "SiO_4" polymerization on Raman intensities. *J. Non-Crystall. Solids* **2013**, *370*, 10–17. [CrossRef]
79. Colomban, P. Glaze and enamels. In *Encyclopedia of Glass Science, Technology, History and Culture*, 1st ed.; Richet, P., Ed.; John Wiley & Sons: Hoboken, NJ, USA, 2020; pp. 1309–1326.
80. Maggetti, M.; d'Albis, A. Phase and compositional analysis of a Sèvres soft paste porcelain platefrom 1781, with a review of early porcelain techniques. *Eur. J. Min.* **2017**, *29*, 347–367. [CrossRef]
81. Hassan, H.K.; Torell, L.M.; Börjesson, L.; Doweidar, H. Structural changes of Be2O3 through the liquid-glass transition range: A Raman-scattering study. *Phys. Rev. B* **1992**, *45*, 12797. [CrossRef]
82. Ciceo-Lucatel, R.; Ardelean, R. FT-IR and Raman study of silver lead borate-based glasses. *J. Non-Crystall. Solids* **2007**, *353*, 2020–2024. [CrossRef]
83. Satyanarayana, T.; Kityk, I.V.; Piasecki, M.; Bragiel, P.; Brik, M.G.; Gandhi, Y.; Veeraiah, N. Structural investigations on PbO–Sb_2O_3–B_2O_3:CoO glass ceramics by means of spectroscopic and dielectric studies. *J. Phys. Condens. Matter* **2009**, *21*, 245104. [CrossRef]
84. Moshkina, E.; Gudim, I.; Temerov, V.; Krylov. Temperature-dependent absorption lines observation in Raman spectra of $SmFe_3(BO_3)_4$ ferroborate. *J. Raman Spectrosc.* **2018**, *49*, 1732–1735. [CrossRef]
85. Préaud, T.; d'Albis, J. *La Porcelaine de Vincennes*; AdamBiro: Paris, France, 1991.
86. Bourgeois, E. *Les Archives de la Manufacture de Sèvres 1741–1905. Unpuplished Report*; Manufacture Nationale: Sèvres, France, 1905; 37p.
87. Doru, T. Chimie Appliquée et Technologie Chimique en France au Milieu du XVIIIe Siècle. Oeuvre et Vie de Jean Hellot. Ph.D. Thesis, Ecole Pratique des Hautes Etudes, Université de Paris-Sorbonne, Paris, France, 1977.
88. Wisniak, J. Jean Hellot. A pioneer of chemical technology. *Revista CENIC Ciencias Quimicas* **2009**, *40*, 111–121.
89. Brongniart, A. Sur les couleurs obtenues des oxides métalliques, et fixées par la fusion sur les différents corpsvitreux. *J. Mines* **1802**, *12*, 58–79.

90. Brongniart, A. *Traité des Arts Céramiques ou des Poteries Considéréesdans leur Histoire, leur Pratique et Leur Théorie*, 2nd ed.; Béchet Jeune: Paris, France, 1854.
91. D'Albis, A. Steps in the manufacture of the soft-paste porcelain of Vincennes, according to the books of Hellot. In *Ancient Technology to Modern Science*; Kingery, W.D., Ed.; Ceramics and Civilization I; American Ceramic Society: Columbus, OH, USA, 1985; pp. 257–271.
92. D'Albis, A. Methods of manufacturing porcelain in Francein the later seventeenth and early eighteenth centuries. In *Discovering the Secrets of Soft-Paste Porcelain at the Saint-Cloud Manufactory ca. 1690–1766*; Rondot, B., Ed.; Yale University Press: New Haven, CT, USA; London, UK,, 1999; pp. 35–42.
93. D'Albis, A. *Traité de la Porcelaine de Sèvres*; Faton: Dijon, France, 2003.
94. Pinto, A.; Sciau, P.; Zhu, T.Q.; Zhao, B.; Groenen, E.S. Raman study of Ming porcelain dark spots: Probing Mn-rich spinels. *J. Raman Spectrosc.* **2019**, *50*, 711–719. [CrossRef]
95. Colomban, P.; Simsek Franci, G.; Kirmizi, B. Cobalt and Associated Impurities in Blue (and Green) Glass, Glaze and Enamel: Relationships between Raw Materials, Processing, Composition, Phases and International Trade. *Minerals* **2021**, *11*, 633. [CrossRef]
96. Sakellariou, K.; Miliani, C.; Morresi, A.; Ombelli, M. Spectroscopic investigation of yellow majolica glazes. *J. Raman Spectrosc.* **2004**, *35*, 61–67. [CrossRef]
97. Sandalinas, C.; Ruiz-Moreno, S. Lead-tin-antimony yellow-Historical manufacture, molecular characterization and identification in seventeenth-century Italian paintings. *Stud. Conserv.* **2004**, *49*, 41–52. [CrossRef]
98. Sandalinas, C.; Ruiz-Moreno, S.; Lopez-Gil, A.; Miralles, J. Experimental confirmation by Raman spectroscopy of a Pb-Sn-Sb triple oxide yellow pigment in sixteenth-century Italian pottery. *J. Raman Spectrosc.* **2006**, *37*, 1146–1153. [CrossRef]
99. Rosi, F.; Manuali, V.; Miliani, C.; Brunetti, B.G.; Sgamellotti, A.; Grygar, T.; Hradil, D. Raman scattering features of lead pyroantimonate compounds. Part I: XRD and Raman characterization of $Pb_2Sb_2O_7$ doped with tin and zinc. *J. Raman Spectrosc.* **2009**, *40*, 107–111. [CrossRef]
100. Ricciardi, P.; Colomban, P.H.; Tournié, A.; Milande, V. Non-destructive on-site identification of ancient glasses: Genuine artefacts, embellished pieces or forgeries? *J. Raman Spectrosc.* **2009**, *40*, 604–617. [CrossRef]
101. Pereira, M.; de Lacerda-Aroso, T.; Gomes, M.J.M.; Mata, A.; Alves, L.C.; Colomban, P.H. Ancient Portuguese ceramic wall tiles ("Azulejos"): Characterization of the glaze and ceramic pigments. *J. Nano Res.* **2009**, *8*, 79–88. [CrossRef]
102. Pelosi, C.; Agresti, G.; Santamaria, U.; Mattei, E. Artificial yellow pigments: Production and characterization through spectroscopic methods of analysis. *e-Preserv. Sci.* **2010**, *7*, 108–115.
103. Rosi, F.; Manuali, V.; Grygar, T.; Bezdicka, P.; Brunetti, B.G.; Sgamellotti, A.; Burgio, L.; Seccaroni, C.; Miliani, C. Raman scattering features of lead pyroantimonate compounds: Implication for the non-invasive identification of yellow pigments on ancient ceramics. Part II. In situcharacterisation of Renaissance plates by portable micro-Raman and XRF studies. *J. Raman Spectrosc.* **2011**, *42*, 407–414. [CrossRef]
104. Cartechini, L.; Rosi, F.; Miliani, C.; D'Acapito, F.; Brunetti, B.G.; Sgamellotti, A. Modified Naples yellow in Renaissance majolica: Study of Pb-Sb-Zn and Pb-Sb-Fe ternary pyroantimonates by X-ray absorption spectroscopy. *J. Anal. At. Spectrom.* **2011**, *26*, 2500–2507. [CrossRef]
105. Colomban, P.; Kırmızı, B.; Zhao, B.; Clais, J.-B.; Yang, Y.; Droguet, V. Investigation of the Pigments and Glassy Matrix of Painted Enamelled Qing Dynasty Chinese Porcelains by Noninvasive On-Site Raman Microspectrometry. *Heritage* **2020**, *3*, 50. [CrossRef]
106. Manoun, B.; Azdouz, M.; Azrour, M.; Essehli, R.; Benmokhtar, S.; El Ammari, L.; Ezzahi, A.; Ider, A.; Lazor, P. Synthesis, Rietveld refinements and Raman spectroscopic studies of tricationic lacunar apatites $Na_{1-x}K_xPb_4(AsO_4)_3$ ($0 < x < 1$). *J. Mol. Struct.* **2011**, *986*, 1–9.
107. Froment, F.; Tournié, A.; Colomban, P. Raman identification of natural red to yellow pigments: Ochre and iron-containing ores. *J. Raman Spectrosc.* **2008**, *39*, 560–568. [CrossRef]
108. Zeynal, O.A.; Jahangirli, Z. First-principles lattice dynamics and Raman scattering in ionic conductor β-Ag2S: Lattice dynamics and Raman scattering in ionic conductor β-Ag_2S. *Phys. Stat. Sol. B* **2016**, *253*, 2049–2055. [CrossRef]
109. Sadovnikov, E.; Vovkotrub, A.; Rempel, S. Micro-Raman Spectroscopy of Nanostructured Silver Sulfide. *Doklady Phys. Chem.* **2018**, *480*, 81–84. [CrossRef]
110. Colomban, N.Q.; Liem, G.; Sagon, H.X.; Tinh, T.B.; Hoành, P. Microstructure, composition and processing of 15th century Vietnamese porcelains and celadons. *J. Cult. Herit.* **2003**, *4*, 187–197. [CrossRef]